NicDaeid Niamh (Orcid ID: 0000-0002-9338-0887)
Sutcliffe Oliver (Orcid ID: 0000-0003-3781-7754)
Stove Christophe (Orcid ID: 0000-0001-9117-4759)
McKenzie Craig (Orcid ID: 0000-0001-7244-5779)

Shape Matters: The Application of Activity-Based *In Vitro* Bioassays and Chiral Profiling to the Pharmacological Evaluation of Synthetic Cannabinoid Receptor Agonists in Drug-Infused Papers Seized in Prisons

Lysbeth H. Antonides[1], Annelies Cannaert[2], Caitlyn Norman[1], Niamh Nic Daeid[1], Oliver B. Sutcliffe[3], Christophe P. Stove[2*], Craig McKenzie[1*]

[1]Leverhulme Research Centre for Forensic Science, University of Dundee, Dundee, United Kingdom, [2]Laboratory of Toxicology, Department of Bioanalysis, Faculty of Pharmaceutical Sciences, Ghent University, Ghent, Belgium, [3]Department of Natural Sciences, Manchester Metropolitan University, Manchester, United Kingdom

Keywords: new psychoactive substances, synthetic cannabinoid receptor agonists, prisons, chiral profiling, activity-based bioassay

Abstract

Synthetic cannabinoid receptor agonists (SCRAs) elicit many of their psychoactive effects via type-1 human cannabinoid (CB_1) receptors. Enantiomer pairs of eight *tert*-leucinate or valinate indole- and indazole-3-carboxamide SCRAs were synthesized and their CB_1 potency and efficacy assessed using an *in vitro* β-arrestin recruitment assay in a HEK239T stable cell system. A chiral high-performance liquid chromatography method with photodiode array and/or quadrupole-time of flight mass spectrometry detection (HPLC-PDA and HPLC-PDA-QToF-MS) was applied to 177 SCRA infused paper samples seized in Scottish prisons between 2018 and 2020. In most samples, SCRAs were almost enantiopure (*S*)-enantiomer (>98% of total chromatographic peak area), although in some (n=18), 2 to 16% of the (*R*)-enantiomer was detected. (*S*)-enantiomers are consistently more potent than (*R*)-enantiomers

This article has been accepted for publication and undergone full peer review but has not been through the copyediting, typesetting, pagination and proofreading process which may lead to differences between this version and the Version of Record. Please cite this article as doi: 10.1002/dta.2965

and often more efficacious. The importance of SCRA-CB_1 receptor interactions in the 'head' or 'linked group' moiety is demonstrated, with the conformation of the 'bulky' *tert*-leucinate group greatly affecting potency (by up to a factor of 374), significantly greater than the difference observed between valinate SCRA enantiomers. (*S*)-MDMB-4en-PINACA, (*S*)-4F-MDMB-BINACA and (*S*)-5F-MDMB-PICA are currently the most prevalent SCRAs in Scottish prisons and all have similar high potency (EC_{50}, 1-5 nM) and efficacy. Infused paper samples were compared using estimated intrinsic efficacy at the CB_1 receptor (EIE_{CB1}) to evaluate samples with variable SCRA content. Given their similar potency and efficacy, any variation in CB_1-receptor mediated psychoactive effects are likely to derive from variation in dose, mode of use, pharmacokinetic differences and individual factors affecting the user, rather than differences in the specific SCRA present.

1. Introduction

Synthetic cannabinoid receptor agonists (SCRAs) are a diverse group of new psychoactive substances (NPS) that exert at least some of their physiological effects *via* binding to, and activation of, the human cannabinoid receptors, CB_1 and CB_2. These are Class A G-Protein-Coupled Receptors (GPCRs)[1-6]; CB_1 receptors are primarily located in the central nervous system and mediate the psychotropic effects of cannabinoids and CB_2 receptors are mainly expressed in the peripheral nervous system, immune system and spleen, and are involved in immunosuppression and analgesia[4,5]. More than 200 SCRAs have been detected on the illicit market to date[7,8], and SCRA intoxications have been reported to cause a variety of adverse effects and have been implicated in drug-related intoxications and deaths worldwide[9-11]. The use of SCRAs, colloquially known as 'Spice' or 'Mamba', in prisons is well documented internationally, particularly in the United Kingdom[12-21]. To facilitate entry into and use within prisons, SCRAs are commonly dissolved in solvents such as acetone and ethanol, infused into papers and cards and sent to prisoners via the mail system. The SCRA-infused papers are vaped using e-cigarettes, particularly where tobacco smoking bans are in place[12,19,21]. The specific SCRA compounds detected over time have continually evolved in response to national and international legislation and availability in source countries. The most prevalent compounds of the last five years have generally been the valinate and *tert*-leucinate indole- and indazole-3-carboxamide SCRAs[12,22,23]. The structures of the SCRAs mentioned are provided in Figure 1 and the bold number in parentheses in the text refers to the numbering provided in this figure. SCRA molecules are commonly described as having four constituent parts: a head or linked group, a linker, a core and tail (see Figure 1 for an example). These compounds include AB-

FUBINACA [*N*-(1-amino-3-methyl-1-oxobutan-2-yl)-1-(4-fluorobenzyl)-1H-indazole-3-carboxamide[**(1)**, MDMB-CHMICA [methyl 2-(1-(cyclohexylmethyl)-1H-indole-3-carboxamido)-3,3-dimethylbutanoate] **(2)**, ADB-FUBINACA [MAB-FUBINACA; methyl (1-(4-fluorobenzyl)-1H-indazole-3-carbonyl)valinate] **(3)**, MMB-FUBINACA [AMB-FUBINACA/FUB-AMB; methyl (1-(4-fluorobenzyl)-1H-indazole-3-carbonyl) valinate] **(4)**, 5F-MDMB-PINACA [5F-ADB; methyl 2-(1-(5-fluoropentyl)-1H-indazole-3-carboxamido)-3,3-dimethyl-butanoate)] **(5)** and, more recently, 5F-MDMB-PICA [5F-MDMB-2201; methyl 2-(1-(5-fluoropentyl)-1H-indole-3-carboxamido)-3,3-di-methylbutanoate] **(6)**, 4F-MDMB-BINACA [Methyl *N*-([1-(4-fluorobutyl)-1H-indazol-3-yl]carbonyl)-3-methyl-*L*-valinate] **(7)** and MDMB-4en-PINACA [5-CL-ADB-A; methyl-3,3-dimethyl-2-(1-(pent-4-en-1-yl)-1H-indazole-3-carboxamido)butanoate] (**8**).

Due to the use of chiral precursors, valinate- and *tert*-leucinate-based SCRAs are chiral compounds; however, it is generally assumed that the SCRAs present in street and prison samples will almost exclusively comprise the (*S*)-enantiomer. This is due to the availability and price of the (*S*)-enantiomers of the chiral precursor compared to those of the (*R*)-enantiomer[24,25] and the greater potency of the (S)-enantiomer final product. Since the precursor used in the final synthetic step (e.g. valinamide and valine methyl ester, for AB- and MMB-compounds respectively, and *tert*-leucinamide and *tert*-leucine methyl ester for ADB- and MDMB-compounds respectively) introduces the chirality into the molecule within the 'head'-group (see Figure 1), it is assumed that the final product is enantiopure. However, there is a possibility that the precursor is not enantiopure, or enantiopure batches of each enantiomer are mixed, resulting in the presence of both enantiomers in the final product. This is important for several reasons: Firstly, the spatial configuration and functionalization of a compound is imperative with regard to receptor binding and activation. Certain functional groups of the SCRA need to interact with specific residues within the orthosteric binding pocket of the cannabinoid receptors in order to activate them[26]. Studying the effects of chirality within the head group on receptor activation will therefore further increase understanding of SCRA-CB_1 receptor interactions in this key region. Secondly, the (*S*)-enantiomers of all compounds tested to date have been shown to be significantly more potent and often more efficacious than their corresponding (*R*)-enantiomers[23,27,28]; therefore, if (*R*)-enantiomers are present in seized samples, they have the potential to lower CB_1 activation-related potency and (potentially) efficacy. Lastly, any variation, if present, in the enantiopurity of valinate and *tert*-leucinate

based SCRAs may provide opportunities to distinguish production batches of drugs which may be useful for intelligence purposes.

SCRAs are produced with an unknown degree of quality assurance of both precursor materials and the finished product, and therefore their enantiopurity and impurity profiles may be subject to some degree of batch-to-batch variation. The use of non-chiral impurity profiling has previously been applied to illicitly produced drugs including heroin[29-31], cocaine[31-34], MDMA[35,36] and fentanyl[37]. Münster-Müller *et al*. describes a novel stable isotope analysis and impurity-profiling workflow, using the SCRAs MDMB-CHMICA **(2)** and Cumyl-5F-PINACA [1-(5-fluoropentyl)-*N*-(2-phenylpropan-2-yl)-1H-indazole-3-carboxamide] **(9)**, for the detection of synthesis precursor/by-product impurities in seized herbal materials and potential source attribution[38-41]. Chiral profiling has been applied previously to illicitly produced drugs including amphetamine and methamphetamine for intelligence purposes[42-44], although the methodology is rarely routinely employed in forensic drug testing laboratories. We suggest that chiral profiling could be applied to chiral valinate and *tert*-leucinate SCRAs in addition to stable isotopic and impurity profiling; however, the potential utility of such chiral profiling is currently unknown as, to date, there have been no large-scale studies to determine the variation of enantiopurity of these SCRAs in seized samples.

Chiral chromatography-based methods are required to determine the variability of enantiopurity in valinate and *tert*-leucinate based SCRAs in drug seizures. The separation of SCRA enantiomers by high pressure liquid chromatography (HPLC) using chiral stationary phases has been reported previously[24,28,44,45]. Doi *et al.* reported the separation and analysis of the enantiomers of 5F-AB-PINACA [*N*-(1-amino-3-methyl-1-oxobutan-2-yl)-1-(5-fluoropentyl)-1H-indazole-3-carboxamide] **(10)** and 5F-MMB-PINACA [5F-AMB/5F-AMB-PINACA; methyl [1-(5-fluoropentyl)-1H-indazole-3-carbonyl]valinate] **(11)** and analyzed 10 street samples[44]. Although the sample size was small, the results indicated that variation in SCRA enantiopurity in seized samples may occur. This method was later expanded to include the separation of five additional carboxamide SCRA enantiomer pairs; however, this expanded method was not applied to seized samples[28]. Andernach *et al.*[45] reported the analysis of five MDMB-CHMICA **(2)** containing herbal samples, all of which were found to contain only (*S*)-MDMB-CHMICA **(2)**, and eight samples containing MDMB-CHMCZCA [methyl *N*-([9-(cyclohexylmethyl)-9H-carbazol-3-yl]carbonyl)-3-methyl-*L*-valinate] **(12)**, in which only one sample was found to contain the (*R*)-enantiomer as a minor component. In our previous study[24].

we demonstrated the chromatographic separation of AB-FUBINACA **(1)**, MMB-FUBINACA **(4)**, 5F-MDMB-PINACA **(5)** and AB-CHMINACA [*N*-(1-amino-3-methyl-1-oxobutan-2-yl)-1-(cyclohexylmethyl)-1H-indazole-3-carboxamide] **(13)** using Lux® Amylose-1 and i-Cellulose-5 chiral HPLC columns and reported the enantiospecific analysis of seized herbal materials containing MMB-FUBINACA **(4)** and 5F-MDMB-PINACA **(5)**.

In this study, we undertook pharmacological profiling of a range of valinate and *tert*-leucinate SCRA enantiomer pairs, using an established CB_1 receptor β-arrestin recruitment-based bioassay[23,24,46-49] to further understand the structural features that influence SCRA potency and efficacy; we expanded the scope of a previously developed chiral HPLC separation method to incorporate a wider range of SCRAs, thereby increasing our understanding of the SCRA-stationary phase interactions[24]; we applied the chiral profiling method to the largest number of SCRA-containing samples tested to date in order to understand the true variability in enantiopurity of SCRAs being used on the illicit market; and finally, we combined the methodologies presented to evaluate the pharmacological impact of the evolution of SCRAs in a continually evolving drugs market in prisons.

2. Materials and Methods

2.1. Materials

All solvents used were HPLC grade (≥ 99.8 % purity) and supplied by either Thermo Fisher Scientific, Loughborough, UK or VWR Chemicals, UK. Ultra-high purity water (18 $M\Omega cm^{-1}$) was obtained using a Milli-Q water purification system (Merck, UK). Reagents necessary for the synthesis of the enantiopure reference standards were obtained from Fluorochem Limited, Hadfield, UK; Sigma-Aldrich, Gillingham, UK; and Alfa Aesar, Heysham, Lancashire, UK, and were used without further purification. D-*tert*-leucine methyl ester was custom synthesized by Carbosynth, UK. Dulbecco's Modified Eagle's Medium (GlutaMAX™), Opti-MEM® I Reduced Serum Medium, Penicillin-Streptomycin (5 000 U/mL) and amphotericin B (250 μg/mL) were purchased from Thermo Fisher Scientific, Loughborough, UK. Fetal bovine serum (FBS) and poly-d-lysine were supplied by Sigma Aldrich, Overijse, Belgium. The Nano-Glo® Live Cell reagent, which was used for the readout of the bioassay, was procured from Promega, Madison, WI, USA.

2.2. Synthesis of SCRA reference standards and characterization by gas chromatography-mass spectrometry (GC-MS) and nuclear magnetic resonance (NMR)

Reference standards for (*R*)- and (*S*)-MMB-FUBINACA **(4)** (>98 % purity) and (*R*)- and (*S*)-5F-MDMB-PINACA **(5)** (99.6 % purity) were obtained via in-house synthesis as detailed previously[24]. Enantiopure reference standards for (*R*)- and (*S*)-5F-MDMB-PICA **(6)**, (*R*)- and (*S*)-4F-MDMB-BINACA **(7)**, (*R*)- and (*S*)-MDMB-4en-PINACA **(8)**, **(***R*)- and (*S*)-5F-MMB-PINACA **(11)**, (*R*)- and (*S*)-MDMB-FUBINACA [*N*-(1-amino-3,3-dimethyl-1-oxobutan-2-yl)-1-(4-fluorobenzyl)-1H-indazole-3-carboxamide] **(14)**, (*R*)- and (*S*)-MMB-CHMICA [AMB-CHMICA; methyl (1-(cyclohexylmethyl)-1H-indole-3-carbonyl)valinate] **(15)**, (*R*)- and (*S*)-MDMB-4en-PICA [methyl 3,3-dimethyl-2-(1-(pent-4-en-1-yl)-1H-indole-3-carboxamido)butanoate] **(16)** and (*R*)- and (*S*)-MMB-4en-PICA [AMB-4en-PICA; MMB-022; methyl (1-(pent-4-en-1-yl)-1H-indole-3-carbonyl)valinate] **(17)** were synthesized as part of this study and synthetic routes, yields and purities are summarized in Table 1. Further details of the synthesis are provided in section 1 of the supplementary information, with the synthesis of MDMB-4en-PINACA provided as an example.

All synthesized reference standards were characterized using GC-MS and NMR spectroscopy (see section 1 of the supplementary information for characterization data) and checked for enantiopurity using a chiral HPLC-photodiode array (PDA) method developed previously and developed further in this study. NMR spectroscopy was performed using a JEOL ECS-400 NMR spectrometer by JEOL, Tokyo, Japan, operating at 400 MHz for ^{1}H-NMR (10 mg/mL in $CDCl_3$) and ^{13}C-NMR (20 mg/mL in $CDCl_3$). NMR purity was calculated using the relative concentration determination method described by Pauli *et al*.[53] GC-MS analysis was performed on an Agilent Technologies 7890B GC system with 5977B MS Detector and 7693 auto sampler by Agilent Technologies, Wokingham, UK, using a capillary column (HP5 MS, 30 m, Å ~ 0.25 mm, i.d. 0.25 μm). Helium was used as a carrier gas at a constant flow rate of 1.0 mL/min. Injection temperature: 270 °C, detection temperature: 300 °C. GC oven: 60 ºC; 10 ºC/min to 300 ºC held for 6 min; transfer line: 295 ºC. Eicosane was used as a retention time marker to ensure that the retention times obtained for the GC-MS analysis of synthesized reference standards were consistent between analysis runs, which was found to be the case. For compounds **(7, 8, 11, 14 & 15)**, methanol was used as the solvent, and for compounds **(6 & 16-17)**, ethyl acetate was used as the solvent.

2.3. Determination of the in vitro biological activity at the cannabinoid receptor 1 (CB_1)

A live cell-based reporter assay, which monitors the *in vitro* CB_1 activation via its interaction with β-arrestin 2 using the NanoLuc Binary Technology, was applied to assess the biological activity of the compounds. Details regarding the development of the stable cell line used here have been reported elsewhere[46,47]. The modified human embryonic kidney (HEK) 293T cells were routinely maintained at 37 °C, 5 % CO_2, under humidified atmosphere in Dulbecco's modified eagle's medium (GlutaMAX™) supplemented with 10 % heat-inactivated FBS, 100 IU/mL of penicillin, 100 µg/mL of streptomycin and 0.25 µg/mL of amphotericin B. For experiments, cells were plated on poly-*D*-lysine coated 96-well plates at 5×10^4 cells/well and incubated overnight. Next, the cells were washed twice with Opti-MEM® I Reduced Serum Medium to remove any remaining FBS, and 100 µL Opti-MEM® I and 25 µL of the Nano-Glo® Live Cell reagent were added to each well. Subsequently, the plate was placed into a TriStar^2 LB 942 multimode microplate reader (Berthold Technologies GmbH & Co., Germany). Luminescence was monitored during the equilibration period until the signal stabilized (15 min). Next, 10 µL per well of test compounds, present as concentrated (13.5-fold, as 10 µL was added to generate a final volume of 135 µL) stock solutions in Opti-MEM® I, was added. The luminescence was continuously monitored for 120 min. Solvent controls were included in all experiments. The results are represented as mean area under the curve (AUC) ± standard error of mean (SEM), obtained in a minimum of three independent experiments, with duplicates run in every experiment. All results were normalized to the E_{max} of JWH-018 (= 100 %), our reference compound. Curve fitting of concentration-response curves via non-linear regression (four-parameter logistic fit) was employed to determine EC_{50} (a measure of potency) and E_{max} (a measure of efficacy) values, using GraphPad Prism software (San Diego, CA, USA).

2.4.1 *Chromatographic separation of SCRA enantiomers*

The development of the chiral separation method utilized here has been described previously[24]. In this study, the method was evaluated for the separation of an expanded range of SCRA enantiomer pairs using the synthesized reference standards. This work was carried out to better understand the separation mechanisms involved, and to better understand the best stationary and mobile phase combinations to resolve enantiomers of SCRAs currently detected in Scottish prisons and to predict the most efficient separation methods for those SCRAs that might emerge in future.

Chiral separations were performed using an Agilent Infinity® II HPLC system with PDA detection (HPLC-PDA, 210 nm). Initial isocratic separations of SCRA enantiomer pairs were carried out using (A) ultra-high purity water (MilliQ H_2O) and (B) acetonitrile (ACN) with a mobile phase composition of 45:55, 50:50 or 55:45 A:B and a flow rate of 0.2 mL/min. To determine column selectivity, 1 or 5 μL of either a 20 or 200 μg/mL SCRA racemic mixture in 50:50 MilliQ H_2O and (B) acetonitrile (ACN) was injected onto either a Lux® Amylose-1 (5 μm, 4.6 × 100 mm) or a Lux® i-Cellulose-5 (5 μm, 4.6 × 100 mm) column (Phenomenex, Macclesfield, UK). Agilent Chemstation software (OpenLab CDS Chemstation Edition rev. C.01.06) was used to assess the chromatographic data, comparing the retention, resolution and peak areas of the enantiomer pairs.

Once the initial method optimization of the HPLC-PDA system was complete, the analytical method was transferred to an HPLC-PDA-quadrupole time of flight (QToF)-MS system using the same chiral columns. A previous study[24] demonstrated that acidification of the mobile phase had little effect on enantiomer resolution and so reference standards and seized sample extracts (see below) were analyzed using an Acquity ultra pressure liquid chromatography (UPLC®) instrument consisting of a binary pump, autosampler (held at 4 °C), vacuum degasser and column oven (held at 30 °C), coupled to a Xevo-QToF-MS/MS system (Waters Corporation, Milford, MA, USA). Mobile phases were (A) LC-MS grade water with 0.1 % formic acid (v/v %) and (B) acetonitrile with 0.1 % formic acid (v/v %) using the same chromatographic conditions as the HPLC-PDA method. The QToF was operated in positive ionization mode with a source temperature of 120 °C, a desolvation temperature at 500 °C and a capillary voltage at 2.25 kV. ToF-MS analysis to determine accurate mass of the SCRA pseudo-molecular ion was carried out with a collision energy at 6 V (scan range 100-1000 Da) and mass error from the theoretical monoisotopic accurate mass calculated. UV spectra (200–400 nm) were collected using an Acquity® PDA detector. MS/MS analysis to provide accurate product ion data was carried out using collision energies ranging from 6 to 28 V (scan range 100-500 Da). The instrument is regularly calibrated against sodium formate clusters using a 5 mM sodium formate solution in 90:10 2-propanol/water and the measured molecular weight was within 1.0 ppm of the theoretical value. The calibration was maintained using a lockspray mass taken at regular intervals during the scan using a leucine-enkephalin lyophilized peptide mixture (Waters Corporation, Milford, MA, USA).

2.5. Selection, collection and storage of seized samples

All seized samples reported in this study were provided by the Scottish Prison Service and were either recovered from incoming mail items or during personal and/or cell searches. Most samples consisted of pieces of paper and card. The seized samples were securely stored in sealed tamperproof polythene evidence bags and all personal information present was removed prior to secure transportation to the laboratory. Transport of samples was overseen by staff from the Police Scotland Drug Expert Witness unit.

2.6. Qualitative analysis of seized samples by GC-MS and UPLC-PDA-QToF-MS

Data originating from the non-chiral qualitative and quantitative analysis of samples seized in three Scottish prisons between 1st June 2018 and 27th September 2019 have been reported previously[12]. The data is reported in this study for completeness in Table S2b in the supplementary information. Sample extracts from the samples prepared for routine qualitative analysis were subsequently used in this chiral profiling study. If not analyzed immediately, sample extracts were frozen at -20 ºC prior to chiral analysis. Additional samples, seized between 28th September 2019 and 12th February 2020 from a single prison (denoted as prison 1 in the original study[12]), were analyzed as part of a long-term longitudinal study to monitor SCRA market evolution in Scottish prisons and this newly reported qualitative data is provided in Table S2b in the supplementary information.

Qualitative analytical methods have been described previously[12]. In brief, two approximately 1 cm^2 samples were cut from opposite corners of the paper sample and placed in a glass vial. To the vial, 0.25 mL methanol was added and the samples sonicated for five minutes. The resulting extract was transferred to a 2 mL amber vial fitted with an insert and analyzed using a 7820A gas chromatograph coupled to a 5977E mass spectrometer from Agilent Technologies, Santa Clara, CA, USA. Injection mode: 1 μL sample injection using a 20:1 split, injection port temperature: 200 ºC, carrier gas: He, flow: 1 mL/min. Column: HP-5MS, 0.33 μm, 0.2 mm x 25 m from Agilent Technologies, Santa Clara, CA, USA. GC oven: 80 ºC held for 3 min; 40 ºC/min to 300 ºC held for 3.5 min; transfer line: 295 ºC. The mass spectrometer operated in electron ionization (EI) mode. Ionization conditions: 70 eV in full scan mode (50–550 Da), ion source: 230 ºC, quadrupole: 150 ºC. SCRAs present in the paper sample extracts were identified by (i) comparing their retention time to reference standards of known origin analyzed under the same conditions within 24 hours of the test sample; (ii) by comparing mass spectra between

the test sample and a reference standard of known origin; and (iii) by comparison of the spectra obtained during the analysis of the sample extract to NIST14, SWGDRUG (v3.5), and Cayman Chemical (versions v04262019 and v09112019) mass spectral libraries with a minimum acceptable reverse match (R-match) value of 850.

The SCRA identifications from the GC-MS analysis were further confirmed by orthogonal analysis using UPLC®-PDA-QToF-MS. Aliquots of the extracts used for GC-MS analysis were diluted 10- or 100-fold in 50:50 MilliQ H_2O:ACN prior to analysis, based upon the GC-MS instrument response for the original extract. When carrying out qualitative SCRA screening using the method described above, highly concentrated SCRA extracts are often produced. The production of such concentrated extracts allows examination of the SCRA impurity profile as part of a separate study, not reported here. Highly concentrated SCRA extracts can cause overloading of the GC column resulting in broad and distorted peaks for the parent SCRAs. If such overloading is observed in the qualitative GC-MS analysis, samples are diluted 100-fold with 50:50 MilliQ H_2O:ACN. If such a high peak area response is not observed on the GC-MS, the sample is diluted 10-fold in 50:50 MilliQ H_2O:ACN. Extract dilution can then be adjusted as required following initial analysis. UPLC-PDA-QToF-MS analysis was performed using an Acquity UPLC® instrument with a binary pump, autosampler held at 4 ºC, vacuum degasser and column oven held at 30 ºC coupled to a Xevo QToF-MS from Waters Corporation, Milford, MA, USA. Mobile phases used were (A) LC-MS grade water with 0.1 % formic acid (v/v %) and (B) ACN with 0.1 % formic acid (v/v %). The gradient used was 50:50 A:B from 0.0-4.0 min, 25:75 A:B from 4.0-5.0 min, 5:95 A:B from 5.0-5.99 min and 50:50 A:B from 6.0-7.0 min. Flow rate was 0.5 mL/min and 1 μL of sample was injected onto an ethylene bridged hybrid (BEH) C_{18} 50 × 2.1 mm, 1.7 μm particle size column (Waters Corporation, Milford, MA, USA). The QToF was operated in positive ionization mode with a source temperature of 120 ºC, a desolvation temperature at 500 ºC and a capillary voltage at 2.25 kV. ToF-MS analysis (scan range 100-1000 Da) for the high-resolution determination of molecular mass was carried out with a collision energy at 6 V. Mass error of the measured accurate mass from theoretical monoisotopic mass was required to be <10 ppm and the UV spectra were compared with reference standards of known origin. Parent ion fragmentation spectra were obtained using MS/MS data acquisition (scan range 100-500 Da) using collision energies between 10 and 30 V for further structural confirmation.

2.7. Chiral profiling of seized sample extracts

Depending on the GC-MS peak area response observed during the original qualitative GC-MS analysis, sample extracts were diluted 10- to 100-fold in 50:50 MilliQ H_2O/ACN and injected using sequential injection volumes of 1 and 5 μL to ensure that, if present, the minor (*R*)-enantiomer of each SCRA was detectable. Further extract dilution adjustments were made to ensure, where possible, a peak height response of greater than 150 absorbance units for the predominant (*S*)-enantiomer. Enantiomer ratios were determined using the relative peak areas (at 210 nm) of the chromatographically resolved enantiomers. Example HPLC-PDA chromatograms for the chiral separation of enantiomer pairs in diluted seized sample extracts are provided in section 3 of the supplementary information. Where chiral HPLC-PDA screening indicated the presence of a SCRA (*R*)-enantiomer >2 % of the peak area of the (*S*)-enantiomer, confirmatory chiral analysis was carried out using the chiral HPLC-PDA-QToF-MS method described earlier. As with the HPLC-PDA screening method, enantiomer ratios were determined using the relative peak areas of the chromatographically resolved enantiomers. Due to its wide linear range, the PDA detector response at 210 nm was used, rather than the TOF-MS or MS/MS response. It was previously found that the calculation of the enantiomer ratio using the MS/MS response led to an over-estimation of the contribution of the minor (*R*)-enantiomer[24]. The ToF-MS and MS/MS data provided confirmation of enantiomer identification in addition to retention time matching to a racemic reference standard.

2.8 Calculation of Estimated Intrinsic Efficacy at the CB_1 receptor (EIE_{CB1}) for SCRAs in infused papers

Estimated Intrinsic Efficacy at the CB_1 receptor (EIE_{CB1}) was calculated using Equation (1) and (2). The calculation utilizes the experimentally derived SCRA efficacy (E_{max}) values (Table 2) relative to the efficacy of the positive control SCRA (JWH-018) which is set to an efficacy of 100% and run with each bioassay experiment. The efficacy data related to the test SCRA and JWH-018 must be taken from the same bioassay experiment to be valid.

$$Estimated\ Intrinsic\ Efficacy_{CB1} = \frac{[Emax_{SCRA,CB1}]}{100}\ x\quad Conc_{SCRA} \qquad (1)$$

When the samples are subjected to chiral analysis and the enantiomer ratio is determined, the following equation can be used, to incorporate this information.

$$Estimated\ Intrinsic\ Efficacy_{CB1} = \frac{[Emax_{SCRA,CB1}\ x\ P(S)] + [Emax_{SCRA,CB1}\ x\ P(R)]}{100}\ x\ Conc_{SCRA} \quad (2)$$

The E_{max} values are in percent, P(*S*) and P(*R*) are the proportions of (*S*)- and (*R*)-enantiomers present and $Conc_{SCRA}$ is the concentration of the SCRA in mg/cm^2 paper. Where a sample contains a mixture of SCRAs, the calculation can be repeated for each SCRA present and the results added together to create a 'mixture' EIE_{CB1}. The results of the calculation for each applicable sample can be found in the supplementary information (Table S2b). Using this method, samples containing multiple SCRAs can be compared in terms of their CB_1-mediated effects, by calculating a total EIE_{CB1} value based on all SCRAs present.

3. Results and Discussion

3.1. Synthesis of the reference standards

To synthesize the sixteen enantiopure carboxamide-type SCRA reference standards, either the method published by Banister *et al.*[50,51] or an adaptation thereof was used, with a shortened scheme shown in Table 1 and further detail provided in section 1 of the supplementary information. This is a three-step reaction, starting from methyl 1*H*-indazole-3-carboxylate for SCRAs with an indazole or from indole for SCRAs with an indole core, respectively. The first step is an alkylation with an alkyl halide, followed by the addition of a trifluoroacetyl group in the case of an indole core. Next is the hydroxylation of the methyl ester group for the indazole compounds and trifluoroacetyl group for the indole compounds. The final step is an amidation using either (*D*-) or (*L*-) *tert*-leucine methyl ester or valine methyl ester. The hydroxylation step was problematic for compounds with an indole core with the use of the hydroxylation method published by Banister *et al*, yielding no product. As an alternative approach, the starting material was dissolved in 20 % sodium hydroxide in water and heated to reflux for 18 h. This was an adaptation of a method reported by Corbett[52] where in a similar compound, the trifluoroacetyl group attached to an indole core was hydrolyzed. This method gave satisfactory yields of 82.3-87.9 % and 81.1-87.3 % for 5F-MDMB-PICA **(6)** and MMB-CHMICA **(15),** respectively. The enantiomers of MDMB-4en-PICA **(16)** and MMB-4en-PICA **(17)** were also prepared using this method, but a lower yield was obtained, due to an isomer impurity which was likely formed from a by-product from the first step which was not sufficiently removed. Further clean-up was required, resulting in a lower yield. The yields and purities of all the

synthesized compounds are provided in Table 1. Enantiomer purity of all synthesized reference standards was assessed as being >99.5% using the chiral HPLC-PDA method described previously.

3.2 In vitro biological activity at CB_1-based receptor bioassay

CB_1 receptors detect extracellular signals through ligand binding and the formation of stabilized ligand-receptor complexes, and transmit these signals across the plasma membrane via receptor conformational changes to evoke a range of cellular responses[54-56]. Like all GPCRs, CB_1 receptors span the plasma membrane of a cell from the extracellular (EC) face to the intracellular (IC) face and comprise seven transmembrane helices (TM). The orthosteric binding site/pocket is on the EC face and there is a G-protein and β-arrestin binding region on the IC face. SCRA binding and receptor activation on the EC domain will induce conformational changes in the SCRA-receptor complex (signal transduction) and these conformational changes will initiate and modulate a variety of downstream signaling pathways which can be measured proximally (as in the *in vitro* β-arrestin recruitment assay used in this study) or alternatively by measuring secondary messengers[23]. GPCRs are known to share common conserved activation mechanisms involving internal hydrogen bonding network rearrangement mediated by structurally conserved water molecules and a well-defined re-orientation of the side-chain conformation of residues within the TM helices[54-57]. Many of these residues are thought to act as molecular switches ('toggle switches' or 'microswitches') and are believed to undergo positional changes upon ligand binding. Current knowledge related to CB receptors has been reviewed recently[6] and two Cryo-EM structures of CB_1-full agonist-Gi protein bound complexes have been solved with MDMB-FUBINACA **(14)**[58] and AM841[59], greatly increasing understanding of CB_1-agonist interactions. Krishna Kumar *et al.* [58] recently solved a CB_1-(*S*)-MDMB-FUBINACA-G_i receptor-ligand complex in its active state and Schoeder *et al.*[60] have carried out a series of CB_1 molecular docking calculations with a wide range of SCRA analogues.

The *in vitro* CB_1 activity data obtained in this study is summarized in Table 2 and provided graphically in section 4 of the supplementary information. Table 2 also includes our previously published data on four related valinate and *tert*-leucinate-3-indazole-carboxamide SCRA enantiomer pairs[24]. Where previously published data on the same compound tested using the same bioassay under similar conditions is available, this data has also been provided for

comparison[23,24,48,49,61]. Consistency and comparability between the SCRAs analyzed in different studies is demonstrated as in most cases the confidence intervals of the potency and efficacy values overlap. As expected, all investigated compounds were able to bind to and activate CB_1 receptors, with (*S*)-enantiomers being consistently more potent than (*R*)-enantiomers. (*S*)-MDMB-FUBINACA **(14)** was the most potent compound tested in this study, with CB_1 activity in the sub-nanomolar range (EC_{50} = 0.245 nM), confirming previous studies indicating that the relative position of the functional groups and the rigid 'C'-shape configuration of the (*S*)-enantiomer of this compound results in high potency[58,60]. This rigid 'C'-shape is also seen in high CB_1 potency γ-carboline PEGACLONE-type SCRAs where the linker group is effectively fused to the core group e.g. Cumyl-PEGACLONE, (EC_{50} = 0.09-0.23 nM)[49,62] and 5F-Cumyl-PEGACLONE (EC_{50} = 0.58 nM)[62]. (*S*)-MMB-4en-PICA **(17)** was the least potent of the (*S*)-enantiomers studied here (EC_{50} = 149 nM) and (*R*)-MMB-4en-PICA **(17)** was the least potent compound of all those tested (EC_{50} = 481 nM).

In vitro CB_1 activation studies using a range of bioassays have consistently shown that compounds with a *tert*-leucine methyl ester head group (MDMB-compounds) are more potent than their valine methyl ester analogues (MMB-compounds)[23,24,50,51,59]. In our data, this is confirmed by comparison of (*S*)-MDMB-FUBINACA **(14**) with (*S*)-MMB-FUBINACA **(4)**, (*S*)-5F-MDMB-PINACA **(5)** with (*S*)-5F-MMB-PINACA **(11)** and (*S*)-MDMB-4en-PICA **(16)** with (*S*)-MMB-4en-PICA **(17)**, and the same comparisons between the equivalent (*R*)-enantiomers in this study (Table 2). Upon SCRA binding, positional changes of the EC faces of TM1 and TM2 have been shown to reduce the volume of the orthosteric ligand-binding site[55,56,58,59]. As a result, the Phe200$^{3.36}$ amino acid residue on TM3 rotates away from residue Trp356$^{6.48}$ on TM6 (the interaction between these two amino acid residues is commonly referred to as the "toggle twin switch"), allowing π–π interactions between the Phe200$^{3.36}$ residue and the indazole core of MDMB-FUBINACA **(14)**, stabilizing the active state-conformation of the receptor. As the Trp356$^{6.48}$ residue is displaced it causes a positional change in the IC end of TM6 in the G-protein binding region, influencing downstream signaling. The methyl ester moiety of MDMB-FUBINACA **(14)** is reported to interact with the His178$^{2.65}$ residue on TM2 and the amide linker with a strongly bound water residue in this region (interactions between His178$^{2.65}$, Ser383$^{7.39}$ and the bound water molecule have been postulated)[52,53,55,56]. Less information is available on the interaction of the other end of the head group (*tert*-butyl or dimethyl moieties) with CB_1 receptor binding pocket residues.

Our CB_1 activity data for *tert*-leucine methyl ester (MDMB-type) and valine methyl ester (MMB-type) SCRA enantiomer pairs, as measured by the in vitro β-arrestin recruitment assay (Table 2 and Figure S4), supports the view that the size and spatial configuration of this part of the SCRA and its interaction with CB_1 receptor residues within the binding pocket has a significant effect on compound potency. The difference in potency between MMB-type enantiomer pairs (*R/S* EC_{50} ratio 3.23-11.6) is significantly lower than the difference in potency of the *tert*-leucine methyl ester MDMB-type enantiomer pairs (*R/S* EC_{50} ratio 74.8-374). This difference may be due to the relative bulk of the *tert*-butyl moiety and its relative inflexibility in interacting with important receptor residues within the CB_1 orthosteric binding pocket. Changes in the orientation of the *tert*-butyl moiety of the MDMB-type SCRAs due to chirality is therefore suggested to have a much greater effect on MDMB-type SCRA-CB_1 residue interactions. The MMB-type SCRAs are likely to have more flexibility within the binding pocket in this region and are therefore able to maintain, at least to some extent, the required receptor residue interactions when the conformation changes from (*S*) to (*R*).

The aromatic core of the SCRA molecules included in this study is likely to be involved in π–π interactions with the Phe200$^{3.36}$ residue, as seen for the agonists MDMB-FUBINACA **(14)**[58] and AM841[59]. In line with previous studies using the same bioassay[23], a cAMP assay[60], and the FLIPR® membrane potential assay [50,51,63] (secondary messenger assays), the potency of the indazoles studied ('INACA' compounds) here are similar to their corresponding indole analogues ('ICA' compounds). This is exemplified by comparison of the EC_{50} value of (*S*)-5F-MDMB-PINACA **(5)** (1.78 nM, from our previous study) with that of the (*S*)-5F-MDMB-PICA **(6)** (2.13 nM, this study) and the EC_{50} values of (*S*)-MDMB-4en-PINACA **(8)** and (*S*)-MDMB-4en-PICA **(16)** (1.11 and 3.70 nM respectively, both this study).

To study the combinational effects of these structural variants (head/core groups), Figure 2a compares the SCRA analogues (*S*)-MDMB-4en-PINACA **(8)**, (*S*)-MDMB-4en-PICA **(16)** and (*S*)-MMB-4en-PICA **(17)**, and demonstrates that (*S*)-MMB-4en-PICA is the least potent of these (EC_{50}, 149 nM) due to the presence of both the isopropyl (MMB) moiety on the head group and a potential additive effect of an indole (I) core. (*R*)-MMB-4en-PICA was the least potent of all the SCRAs tested in the study, demonstrating the even greater effect of chirality in reducing the potency (EC_{50}, 481 nM). In terms of efficacy, with the exception of MMB-

CHMICA **(15)** and 5F-MMB-PINACA **(11)**, all (*S*)-enantiomers were more efficacious than their corresponding (*R*)-enantiomers, as noted in our previous study[24]. MMB-CHMICA **(15)** and 5F-MMB-PINACA **(11)** have the same maximal response (efficacy) for both enantiomers. This may occur as a result of the β-arrestin recruitment assay reaching its maximal receptor reserve[64,65] meaning that the assay cannot differentiate them, which in turn indicates that these compounds are particularly efficacious. The receptor reserve effect is, however, more commonly observed in CB_1 assays measuring secondary messengers (e.g. cAMP, FLIPR, etc.) than in assays measuring more proximal signaling pathways, such as β-arrestin recruitment or G-protein activation[23]. Therefore, this finding requires further investigation.

The assay data for the (*S*)-enantiomers of the currently most prevalent SCRAs in Scottish prisons (5F-MDMB-PICA **(6)**, 4F-MDMB-BINACA **(7)** and MDMB-4en-PINACA **(8)**) are compared in Figure 2b, demonstrating that, as highly potent and efficacious CB_1 agonists, they are all likely to have similar CB_1-mediated effects if consumed in the same manner (e.g. vaping) by the same user at the same concentration and if they have similar pharmacokinetic properties. This assessment does not, however, account for any effects of these substances which are not mediated via the CB_1 receptor.

3.3. Chiral separation of valinate and tert-leucinate indole- and indazole-3-carboxamide SCRA enantiomers

We previously described the development of a method for the separation of the enantiomers of AB-FUBINACA **(1)**, MMB-FUBINACA **(4)**, 5F-MDMB-PINACA **(5)** and AB-CHMINACA **(13)** using Lux® Amylose-1 and Lux® i-Cellulose-5 chiral HPLC columns[24]. The selectivity of the same chiral columns for the eight additional SCRA enantiomer pairs synthesized in this study was investigated. Chromatograms showing the optimum separation of each enantiomer pair are provided in section 3 of the supplementary information. Enantiomers of the *tert*-leucine methyl ester compounds (MDMBs) with indazole cores, 4F-MDMB-BINACA **(7)**, MDMB-4en-PINACA **(8)** and MDMB-FUBINACA **(14)**
were all resolved at 50:50 and 55:45 MilliQ H_2O:ACN on the Lux® Amylose-1 column and all but 4F-MDMB-FUBINACA were resolved at 45:55 MilliQ H_2O:ACN with MDMB-FUBINACA enantiomers demonstrating the greatest retention (Figure S5a). As noted previously[24], 5F-MDMB-PINACA **(5)** enantiomers, like 4F-MDMB-BINACA **(7)**

enantiomers, were resolved at both 50:50 and 55:45 MilliQ H_2O:ACN and the chromatograms are provided in the supplementary information for reference (Figure S5a).

The *tert*-leucine methyl ester (MDMB-type) indole-3-carboxamides, 5F-MDMB-PICA **(6)** and MDMB-4en-PICA **(16)** (Figure S5b), were close to being resolved on the Lux® Amylose-1 column, but only at 55:45 MilliQ H_2O:ACN, indicating the role of the core moiety in the chiral separation mechanism.

Of the valine methyl ester SCRAs, the enantiomers of MMB-FUBINACA **(4)**, with an indazole core and a fluorobenzyl tail, were resolved on the Lux® Amylose-1 column at 50:50 and 55:45 H_2O:ACN (Figure S5c) as reported previously[24]. Enantiomers of 5F-MMB-PINACA **(11)**, a valine methyl ester SCRA with an indazole core and a terminal fluorine, was not fully resolved at 55:45 H_2O:ACN (Figure S5c). The enantiomers of the remaining valine methyl ester SCRAs with indole cores included in this study, MMB-CHMICA **(15)** and MMB-4en-PICA **(17)**, were not resolved on the Lux® Amylose-1 column. The Lux® i-Cellulose-5 column resolved the enantiomers of MMB-CHMICA **(15)** and MMB-4en-PICA **(17)** at 55:45 H_2O:ACN, although the elution order was reversed, with the (*S*)-enantiomer eluting before the (*R*)-enantiomer (Figure S5d). The resolution of the other SCRAs was not improved from that achieved with the Lux® Amylose-1 column and the elution order did not change (data not shown).

The chiral selector requires a three-point interaction with the SCRA for optimum separation efficiency. For the Lux® Amylose-1 stationary phase, selectivity is optimized for those SCRAs with a bulky *tert*-butyl moiety on the head group (MDMB-type SCRAs), an indazole core and increased electronegativity/π-electron density in the tail group (e.g. fluorobenzyl group > alkene > terminal fluorine). For the Lux® i-Cellulose-5 column, selectivity is optimized for SCRAs with a less bulky isopropyl head group (MMB-type compounds) and the elution order is reversed for SCRAs with the MMB-type head group and an indole core.

3.4. Qualitative analysis of prison-sourced infused paper samples

Sample information and analytical data for the SCRA infused papers included in this study are provided in Table S2b of the supplementary information. Non-chiral data related to samples seized in three Scottish prisons between 1st June 2018 and 27th September 2019 has been reported previously[12] and qualitative and quantitative analytical data is included here for

reference. Infused papers and cards seized between 28th September 2019 and 12th February 2020 from a single Scottish prison (prison 1) are reported in this study for the first time. These samples originated from the analysis of 86 separate seizures, comprising 98 individual paper/card samples (within a single seizure, there were often multiple paper/card samples; samples with similar visual characteristics, e.g. paper/card type, ink/handwriting style, etc. were treated as single samples and sampled accordingly). Of the 86 new seizures examined, 45 were found to include papers and cards infused with SCRAs (63 individual paper samples, data provided in Table S2b), 38 seizures contained no controlled drug and trace levels of non-SCRA controlled drugs were found on 3 paper samples (cocaine, amphetamine and ketamine/2-fluorodeschloroketamine; data not shown). The previously observed market evolution from 5F-MDMB-PINACA **(5)** to 5F-MDMB-PICA **(6)** and 4F-MDMB-BINACA **(7)**, then to 4F-MDMB-BINACA (**7**) and MDMB-4en-PINACA (**8**) between June 2018 and 22nd September 2019[12] continued between 28th September 2019 and 12th February 2020. During this period, in prison 1, MDMB-4en-PINACA **(8)** was the most detected SCRA, either alone or in mixtures with 4F-MDMB-BINACA **(7)**, 5F-MDMB-PICA **(6)** or both. A comparison of the previously reported and newly reported data from prison 1 over the two time periods is summarized graphically in section 6 of the supplementary information.

3.5. Chiral profiling of seized samples containing SCRAs

From 1 June 2018 to 12 February 2020, 177 SCRA seized paper samples originating from 126 seizures from three Scottish prisons were analyzed by chiral HPLC-PDA. Chiral profiling was carried out on available paper sample extracts shown by qualitative analysis to contain MMB-FUBINACA **(4)** (n=5), 5F-MDMB-PINACA **(5)** (n=40), 5F-MDMB-PICA **(6)** (n=58), 4F-MDMB-BINACA **(7) (**n=60) and MDMB-4en-PINACA **(8)** (n=47), bearing in mind that some infused paper extracts contained multiple SCRAs. The percentage of (*R*)- and (*S*)-enantiomers detected is provided in the supplementary information (Table S2b) and for those samples where the seizure date was available (n=159), is shown in Figure 3. The majority of the SCRAs analyzed in this study from seized infused papers were, for all intents and purposes, present in an enantiopure form (>98 % (*S*)-enantiomer), consistent with data from previous studies[44,45,66]. The (*S*)-*tert*-leucine methyl ester chiral precursor of the MDMB-type SCRAs in this study is widely available and produced efficiently on an industrial scale with a high degree of reported enantiopurity (>99 %)[25]. However, in 18 of the 210 (8.6 %) individual SCRA enantiomer pair analyses of the samples carried out, the proportion of the (*R*)-enantiomer was higher than 2 % of the total enantiomer pair peak area. Of these, 11 samples contained 4F-MDMB-BINACA

(7), 5 contained MMB-FUBINACA **(4)** and 2 contained 5F-MDMB-PINACA **(5)**. Of the 4F-MDMB-BINACA **(7)** containing samples, proportions of the (*R*)-enantiomer ranged from 2.2 to 16.2 %. Example chiral chromatograms from seized samples containing higher proportions of (*R*)-4F-MDMB BINACA **(7)** are provided in Figure 4a and 4b. Figure 4a shows the HPLC-PDA chromatogram for sample FL19/0129 in 50:50 MilliQ H_2O:ACN; the green chromatogram relates to a 1μL injection and the blue chromatogram relates to a 5 μL injection. Figure 4b shows an overlay of two samples, which both contain 4F-MDMB-BINACA. The green chromatogram depicts the same sample as in Figure 4a, which contains 11.9 % (*R*)-enantiomer. The blue chromatogram depicts sample FL19/0215-G, which also contains 4F-MDMB-BINACA, but only 0.4 % (*R*)-enantiomer is present. This shows the enantiomeric variability in seized samples. Chromatograms and spectra showing the comparison of a seized sample extract with an (*R*)-enantiomer higher than 2 % of the (*S*)-enantiomer with a racemic 4F-MDMB-BINACA **(7)** reference standard is provided in section 3a-b of the supplementary information, along with further examples of chiral analysis results (supplementary information section 3c-f).

The reason for this enantiomeric variability uncommon, but potentially significant variation in enantiopurity may be the utilization of different batches of precursor material with varying enantiopurity in the synthesis. One possibility for this variation in enantiopurity is that the enantiomeric starting material was not pure, or that a mix of the (*R*)- and (*S*)-enantiomers was used. Variation in enantiopurity of SCRAs in seized samples has been reported previously, notably by Doi *et al.*[44] who analyzed 11 seized herbal samples containing 5F-AB-PINACA **(10)** and 5F-MMB-PINACA **(11)**. Of the 11 samples tested, 9 were enantiopure, containing only the (*S*)-enantiomer, however, two samples contained 13.7 and 10.2 % of the (*R*)-enantiomer respectively. Taken together, this data indicates that there is some meaningful variation in the enantiopurity of SCRAs in seized samples, which could potentially be used for batch profiling purposes, especially when the presence of the (*R*)-enantiomer to any extent is so unexpected.

3.6. Pharmacological evaluation of SCRA-infused papers seized in Scottish prisons

To the best of our knowledge, users of SCRAs in prisons are unaware of the specific compounds present in the infused papers they are vaping, have no indication of the potency compared to previous compounds they have been exposed to and have no way of knowing the

concentration of drug present or the 'appropriate' dosage unit (area of paper used in the e-cigarette) to obtain a desired effect. Norman *et al.*[12] showed that SCRA concentrations vary between infused papers (<0.05-1.17 mg/cm^2), with lower concentrations likely to be present due to cross contamination of SCRA-infused papers and non-infused papers in sample bags, and concentrations were found to vary considerably across infused sheets of paper, depending on how they are prepared.

Previously, we proposed a method of calculating the estimated intrinsic potency (EIP_{CB1}) to compare the potential CB_1-mediated harms of seized samples. This methodology used the potency of each SCRA (EC_{50}) at CB_1 relative to the potency of a reference compound (in this case, JWH-018), the concentration of the SCRA present and its enantiopurity[24]. To calculate the EIP_{CB1} for this set of SCRA-infused papers, we would need to combine the potency data from two studies (this study and Antonides *et al.* [24]). However, as also seen in other studies[46,48,49], there can be an intrinsic variability in the EC_{50} value obtained for the reference (i.e. JWH-018). In this case, despite the EC_{50} values for JWH-018 being of the same order of magnitude (Table 1: 14.2 *vs.* 45.1 nM; Figure 2b), the difference between both obtained values would have a profound impact when using them as a comparator in the previously proposed EIP calculation. The use of (relative) efficacy data (E_{max}) to calculate the estimated intrinsic efficacy at the CB_1 receptor (EIE_{CB1}) might prove to be more robust for the proposed calculations, as the E_{max} of the reference compound will always be set at 100 %, and therefore, the data of distinct studies will be compatible and more easily comparable. Another reason to opt for using E_{max} values was derived from recent insights into opioid signaling, where *in vitro* efficacy was found to better correlate with *in vivo* (side) effects, the efficacy being inversely correlated with the therapeutic window[67-70]. The equations for calculating the EIE_{CB1} values are provided in the methods section (section 2.8).

Data for 112 samples from three Scottish prisons sampled between June 2018 and September 2019, for which both concentration data (from a previous study[12]) and chiral profiling data (from this study) are available, were used to calculate EIE_{CB1} values (see Table S2b in the supplementary information).

Where qualitative analysis (which uses 2 x 1 cm^2 paper sample area) detected a particular SCRA, but the qualitative method (which uses a 3 mm diameter punched paper sample) gave a result below the limit of quantitation (LOQ), a value equal to half of the LOQ was used for

the calculation. LOQs ranged from 0.05-0.09 mg/cm^2 paper, calculated as previously described[12].

The concentrations of the individual SCRAs (<0.05-1.17 mg/cm^2 paper) detected in these 112 samples are described in Figure 5a and Figure 5b summarizes the calculated EIE_{CB1} values. This provides a comparison of the intrinsic efficacy of samples containing different SCRAs or mixtures of SCRAs in the same sample. As shown by the data in Figure 5b, it is likely that all samples would give rise to similar CB_1-mediated effects, due to their similar concentration ranges and similar high efficacy, if the dose (the amount of infused paper used and the concentration of SCRAs present) was kept constant and their pharmacokinetic properties were similar.

Variability of the CB_1-mediated effects experienced by a user may therefore be more influenced by the (unpredictable) dose taken, the mode of use and individual physiological factors, rather than the differences in the SCRA compounds present on the paper. The presence of multiple SCRAs in the same infused paper sample, at least in the mixtures observed in this study, does not give rise to higher sample estimated intrinsic efficacy.

The presence of a relatively small proportion of the (*R*)-enantiomer of a highly potent SCRA compound (e.g. with EC_{50} = 0.1-10 nM) is likely to have little to no impact on the pharmacological effects of vaping SCRA-infused papers. For example, sample FL19/0129, seized in prison 3 (see Table S2b in the supplementary information for further details), contains 0.47 mg/cm^2 4F-MDMB-BINACA **(7)**, of which 11.9 % is the (*R*)-enantiomer. This would theoretically cause a relative reduction of 6 % in estimated intrinsic efficacy at the CB_1 receptor compared to a sample containing only the (*S*)-enantiomer. This is likely to be of little toxicological or pharmacological significance due to the high intrinsic potency of the (*S*)-enantiomer. In samples that contain SCRA mixtures, the influence of the presence of the (*R*)-enantiomer of one of the compounds will have even less of an influence. For example, sample FL19/0207-2 contains 0.47 mg/cm^2 of 5F-MDMB-PICA **(6)**, which is essentially enantiopure (99.5 % (*S*)-enantiomer), and 0.11 mg/cm^2 of 4F-MDMB-BINACA **(7),** with 16.2 % of the (*R*)-enantiomer present. In this case the presence of the (*R*)-enantiomer theoretically reduces the overall total efficacy of the sample by only 1.4 %, with little or no toxicological or pharmacological significance.

Previously published data[12], and the more recent data present in this study, have demonstrated that SCRA compounds present in infused papers in Scottish prisons have changed over time. They are likely to continue to evolve in the future due to the availability and prevalence of particular SCRAs on the wider illicit drugs market. Understanding this evolving SCRA market in a wider context helps to maintain and future-proof screening methods used to detect SCRAs in incoming mail and limit and disrupt supply into prisons. Additionally, it can also enable prediction of the potential for harm from emerging drug threats, allowing a pre-emptive evaluation of potential risk to prisoners and prison staff based on the available information on their pharmacology. Of the most prevalent compounds currently detected in Scottish prisons, 5F-MDMB-PICA **(6)** and 4F-MDMB-BINACA **(7)**, but not MDMB-4en-PINACA **(8)**, are scheduled for international control in November 2020[71]. 5F-MDMB-PINACA **(5)** was controlled by the People's Republic of China in September 2019, leading to its effective disappearance from Scottish prisons a few months later[12]. Based on past experience, if such control is replicated in source/producer jurisdictions, these SCRAs are likely to disappear rapidly from the Scottish prison market, to be replaced with other, less well-studied emerging SCRAs. For example, new valinate and *tert*-leucinate indazole-3-carboxamide compounds continue to be detected. 4F-MDMB-BICA [methyl 2-(([1-(4-fluorobutyl)-1H-indol-3-yl]carbonyl)amino)-3,3-dimethylbutanoate], the indole analogue of 4F-MDMB-BINACA **(7)**; 5F-EMB-PICA [ethyl 2-([1-(5-fluoropentyl)indole-3-carbonyl]amino)-3-methyl-butanoate], an analogue of 5F-MDMB-PICA **(6)**; and MMB-4en-PICA **(17)**, included in this study as an emerging compound, have been seized and reported to early warning systems in the United States[72-74] and Europe[75,76]. 5F-EMB-PICA and 4F-MDMB-BICA have been detected in Scottish prisons for the first time in May 2020[77]. Using the available CB_1 receptor structure-activity relationship (SAR) data for this class of SCRAs, we can begin to pre-emptively evaluate/predict the relative potential for CB_1-mediated harms of emerging compounds. This approach should be supported using *in silico* tools and utilizing the available ground-truth *in vitro* datasets to predict the pharmacological profiles of emerging and yet to emerge SCRA compounds.

4. Conclusions

Sixteen enantiopure SCRA reference standards (eight enantiomer pairs) were synthesized. The potency of each enantiomer was determined using an established CB_1 activity-based bioassay. For all enantiomer pairs, the (*S*)-enantiomer was more potent (EC_{50}, 0.245-149 nM) than the (*R*)-enantiomer (EC_{50}, 76.4-1076 nM). The study provides additional information on the likely

interaction such SCRAs have with the orthosteric binding site of the CB_1 receptor and has further illustrated the importance of the size and spatial orientation of the 'head' group of these compounds in determining their potency and efficacy. The difference in potency, as determined by an in vitro bioassay, between enantiomers is greatest when the bulky *tert*-butyl moiety is present (MDMB-type SCRAs). Using an expanded chiral chromatography method, this study identified some variation in enantiopurity in a small number of samples with up to 16.2 % of the (*R*)-enantiomer of 4F-MDMB-BINACA **(7)** being detected in one sample. This indicates the potential for chiral profiling to be included as a supplementary batch profiling technique to be applied in future to seized and test purchased SCRAs. Combining analytical and pharmacological data, the concept of estimated intrinsic efficacy (EIE_{CB1}) was applied to SCRA-infused papers seized in Scottish prisons allowing some comparison of the likely CB_1-mediated effects between samples containing different SCRA compounds, and in some cases mixtures of SCRA compounds. This approach indicated that whilst the individual SCRAs detected in Scottish prisons may evolve over time, all compounds detected recently have similar high potency and efficacy, and are likely to cause similar CB_1-mediated effects. Increased harms may therefore be predicted if the dose of the SCRAs increased (prisoners taking larger paper samples for vaping) or the concentrations present increased or even higher potency SCRAs emerged without a concurrent decrease in concentration. Increased knowledge of CB_1 receptor-related SARs for SCRAs, together with an understanding of the concentrations of SCRAs present in infused papers alone or in mixtures, allows pre-emptive evaluation of the potential harms of newly emerging compounds in custodial settings.

Acknowledgement

We gratefully acknowledge the Leverhulme Trust who provided funding for L.H. Antonides. The authors are grateful for the support of the Scottish Prison Service. We thank the staff of the Dundee team of the Drug Expert Witness Unit, Police Scotland for the transfer of seized samples from the Scottish Prison Service to the University of Dundee. We acknowledge Prof. U. Zachariae and N. Thompson, Computational Biology, School of Life Sciences, University of Dundee for discussions relating to GPCR activation and signal transduction and Dr. Darren Edwards and Dr. Yoko Shishikura, Drug Discovery Unit, School of Life Sciences, University of Dundee for UPLC-PDA-QToF-MS support. A. Cannaert acknowledges funding as a postdoctoral research fellow from the Research Foundation-Flanders (FWO; 12Y9520N). C. Stove acknowledges funding from the Ghent University - Special Research Fund (Grants No. 01N00814 and No. 01J15517).

Supplementary Information

Electronic Supplementary Information to this article can be found online at:

References

1. Matsuda LA, Lolait SJ, Brownstein MJ, Young AC, Bonner TI. Structure of a cannabinoid receptor and functional expression of the cloned cDNA. *Nature.* 1990;346(6284):561-564, doi:https://doi.org/10.1038/346561a0.
2. Munro S, Thomas KL, Abu-Shaar M. Molecular characterization of a peripheral receptor for cannabinoids. *Nature.* 1993;365(6441):61-65, doi:https://doi.org/10.1038/365061a0.
3. Pertwee RG. Pharmacology of cannabinoid CB_1 and CB_2 receptors. *Pharmacol Ther.* 1997;74(2):129-180, doi:https://doi.org/10.1016/s0163-7258(97)82001-3.
4. Pertwee RG, Howlett A, Abood ME, et al. International union of basic and clinical pharmacology. LXXIX. Cannabinoid receptors and their ligands: beyond CB_1 and CB_2. *Pharmacol Rev.* 2010;62(4):588-631, doi:https://doi.org/10.1124/pr.110.003004.
5. Mechoulam R, Parker LA. The endocannabinoid system and the brain. *Annu Rev Psychol.* 2013;64:21-47, doi:https://doi.org/10.1146/annurev-psych-113011-143739.
6. Shahbazi F, Grandi V, Banerjee A, Trant JF. Cannabinoids and cannabinoid receptors: The story so far. *iScience.* 2020:101301, doi:https://doi.org/10.1016/j.isci.2020.101301.
7. European Monitoring Centre for Drugs and Drug Addiction. *European Drug Report 2019, Trends and developments.* Luxembourg: Publications Office of the European Union;2019, doi:https://doi.org/10.2810/191370.
8. Potts A, Cano C, Thomas S, Hill S. Synthetic cannabinoid receptor agonists: classification and nomenclature. *Clinical Toxicology.* 2020;58(2):82-98, doi:https://doi.org/10.1080/15563650.2019.1661425.
9. Trecki J, Gerona RR, Schwartz MD. Synthetic cannabinoid-related illnesses and deaths. *N Engl J Med.* 2015;373(2):103-107, doi:https://doi.org/10.1056/NEJMp1505328.
10. Luethi D, Liechti ME. Designer drugs: Mechanism of action and adverse effects. *Arch Toxicol.* 2020:1-49, doi:https://doi.org/10.1007/s00204-020-02693-7.
11. Giorgetti A, Busardò FP, Tittarelli R, Auwärter V, Giorgetti R. Post-mortem toxicology: A systematic review of death cases involving synthetic cannabinoid receptor agonists. *Front Psychiatry.* 2020;11, doi:https://doi.org/10.3389/fpsyt.2020.00464.
12. Norman C, Walker G, McKirdy B, et al. Detection and quantitation of synthetic cannabinoid receptor agonists in infused papers from prisons in a constantly evolving illicit market. *Drug Test Anal.* 2020;12(4):538-554, doi:https://doi.org/10.1002/dta.2767.
13. Ralphs R, Williams L, Askew R, Norton A. Adding spice to the porridge: The development of a synthetic cannabinoid market in an English prison. *Int J Drug Policy.* 2017;40:57-69, doi:https://doi.org/10.1016/j.drugpo.2016.10.003.
14. HM Prison & Probation Service. *Her Majesty's prison and probation service annual report and accounts 2018-19.* 2019 Available from: https://assets.publishing.service.gov.uk/government/uploads/system/uploads/attachment_data/file/818788/HMPPS_Annual_Report_and_Accounts_2018-19__web_.pdf. Accessed: 06-06-2020

15. European Monitoring Centre for Drugs and Drug Addiction. *New Psychoactive Substances in Prison: Results from an EMCDDA Trendspotter Study.* Luxembourg: Publications Office of the European Union;2018, doi:https://doi.org/10.2810/492880.
16. Scottish Prison Service. *Scottish prison service annual report and accounts 2017-2018.* 2018 Available from: http://www.sps.gov.uk/Corporate/Publications/Publication-6017.aspx. Accessed: 06-06-2020
17. National Offender Management Service. *North West 'Through the gate substance misuse services' drug testing project – further public health monitoring study – North West final report.* 2015 Available from: https://www.lgcgroup.com/media/1795/noms-final-phm-report-version-5.pdf. Accessed: 06-06-2020
18. Grace S, Lloyd C, Perry A. The spice trail: transitions in synthetic cannabis receptor agonists (SCRAs) use in English prisons and on release. *Drugs (Abingdon Engl).* 2019:1-11, doi:https://doi.org/10.1080/09687637.2019.1684878.
19. Ford LT, Berg JD. Analytical evidence to show letters impregnated with novel psychoactive substances are a means of getting drugs to inmates within the UK prison service. *Ann Clin Biochem.* 2018;55(6):673-678, doi:https://doi.org/10.1177/0004563218767462.
20. Hvozdovich JA, Chronister CW, Logan BK, Goldberger BA. Case report: synthetic cannabinoid deaths in state of Florida prisoners. *J Anal Toxicol.* 2020;44(3):298-300, doi:https://doi.org/10.1093/jat/bkz092.
21. Caterino J, Clark J, Yohannan JC. Analysis of synthetic cannabinoids on paper before and after processing for latent print using DFO and ninhydrin. *Forensic Sci Int.* 2019;305:110000, doi:https://doi.org/10.1016/j.forsciint.2019.110000.
22. Banister SD, Connor M. The chemistry and pharmacology of synthetic cannabinoid receptor agonists as new psychoactive substances: origins. In: *New psychoactive substances.* Springer; 2018:165-190, doi:https://doi.org/10.1007/164_2018_143.
23. Wouters E, Mogler L, Cannaert A, Auwärter V, Stove C. Functional evaluation of carboxy metabolites of synthetic cannabinoid receptor agonists featuring scaffolds based on L-valine or L-*tert*-leucine. *Drug Test Anal.* 2019;11(8):1183-1191, doi:https://doi.org/10.1002/dta.2607.
24. Antonides LH, Cannaert A, Norman C, et al. Enantiospecific synthesis, chiral separation, and biological activity of four indazole-3-carboxamide-type synthetic cannabinoid receptor agonists and their detection in seized drug samples. *Front Chem.* 2019;7(321), doi:https://doi.org/10.3389/fchem.2019.00321.
25. Xue Y-P, Cao C-H, Zheng Y-G. Enzymatic asymmetric synthesis of chiral amino acids. *Chem Soc Rev.* 2018;47(4):1516-1561, doi:https://doi.org/10.1039/C7CS00253J.
26. McConathy J, Owens MJ. Stereochemistry in drug action. *Primary Care Companion to The Journal of Clinical Psychiatry.* 2003;5:70-73, doi:https://doi.org/10.4088/pcc.v05n0202.
27. Buchler IP, Hayes MJ, Hedge SG, et al., Inventors; Pfizer Inc., assignee. INDAZOLE DERIVATIVES. US patent WO/2009/1069822009. Available at: https://patents.google.com/patent/WO2009106982A1/en.
28. Doi T, Tagami T, Takeda A, Asada A, Sawabe Y. Evaluation of carboxamide-type synthetic cannabinoids as CB1/CB2 receptor agonists: difference between the enantiomers. *Forensic Toxicol.* 2018; 36:51-60, doi:https://doi.org/10.1007/s11419-017-0378-5.

29. Dufey V, Dujourdy L, Besacier F, Chaudron H. A quick and automated method for profiling heroin samples for tactical intelligence purposes. *Forensic Sci Int.* 2007;169(2-3):108-117, doi:https://doi.org/10.1016/j.forsciint.2006.08.003.
30. Schwemer T, Rössler T, Ahrens B, et al. Characterization of a heroin manufacturing process based on acidic extracts by combining complementary information from two-dimensional gas chromatography and high resolution mass spectrometry. *Forensic Chem.* 2017;4:9-18, doi:https://doi.org/10.1016/j.forc.2017.02.006.
31. Popovic A, Morelato M, Roux C, Beavis A. Review of the most common chemometric techniques in illicit drug profiling. *Forensic Sci Int.* 2019;302:109911, doi:https://doi.org/10.1016/j.forsciint.2019.109911.
32. Nielsen LS, Villesen P, Lindholst C. Variation in chemical profiles within large seizures of cocaine bricks. *Forensic Sci Int.* 2017;280:194-199, doi:https://doi.org/10.1016/j.forsciint.2017.10.007.
33. Materazzi S, Gregori A, Ripani L, Apriceno A, Risoluti R. Cocaine profiling: Implementation of a predictive model by ATR-FTIR coupled with chemometrics in forensic chemistry. *Talanta.* 2017;166:328-335, doi:https://doi.org/10.1016/j.talanta.2017.01.045.
34. Villesen P, Nielsen LS. Profiling of cocaine using ratios of GC-MS peaks. *Sci Rep.* 2017;7(1):1-8, doi:https://doi.org/10.1038/s41598-017-12042-x.
35. Milliet Q, Weyermann C, Esseiva P. The profiling of MDMA tablets: a study of the combination of physical characteristics and organic impurities as sources of information. *Forensic Sci Int.* 2009;187(1-3):58-65, doi:https://doi.org/10.1016/j.forsciint.2009.02.017.
36. Heather E, Shimmon R, McDonagh A. Organic impurity profiling of 3, 4-methylenedioxymethamphetamine (MDMA) synthesised from catechol and eugenol via 4-allylcatechol. *Forensic Sci Int.* 2020;309:110176, doi:https://doi.org/10.1016/j.forsciint.2020.110176
37. Mörén L, Qvarnström J, Engqvist M, et al. Attribution of fentanyl analogue synthesis routes by multivariate data analysis of orthogonal mass spectral data. *Talanta.* 2019;203:122-130, doi:https://doi.org/10.1016/j.talanta.2019.05.025.
38. Münster-Müller S, Hansen S, Opatz T, Zimmermann R, Pütz M. Chemical profiling of the synthetic cannabinoid MDMB-CHMICA: Identification, assessment, and stability study of synthesis-related impurities in seized and synthesized samples. *Drug Test Anal.* 2019;11(8):1192-1206, doi:https://doi.org/10.1002/dta.2652.
39. Münster-Müller S, Matzenbach I, Knepper T, Zimmermann R, Pütz M. Profiling of synthesis-related impurities of the synthetic cannabinoid Cumyl-5F-PINACA in seized samples of e-liquids via multivariate analysis of UHPLC− MSn data. *Drug Test Anal.* 2020;12(1):119-126, doi:https://doi.org/10.1002/dta.2673.
40. Münster-Müller S, Scheid N, Zimmermann R, Pütz M. Combination of stable isotope ratio data and chromatographic impurity signatures as a comprehensive concept for the profiling of highly prevalent synthetic cannabinoids and their precursors. *Anal Chim Acta.* 2020;1108:129-141, doi:https://doi.org/10.1016/j.aca.2020.01.029.
41. Münster-Müller S, Zimmermann R, Pütz M. A novel impurity-profiling workflow with the combination of flash-chromatography, UHPLC-MS, and multivariate data analysis for highly pure drugs: a study on the synthetic cannabinoid MDMB-CHMICA. *Anal Chem.* 2018;90(17):10559-10567, doi:https://doi.org/10.1021/acs.analchem.8b02679.
42. Wang T, Yu Z, Shi Y, Xiang P. Enantiomer profiling of methamphetamine in white crystal and tablet forms (ma old) using LC–MS-MS. *J Anal Toxicol.* 2015;39(7):551-556, doi:https://doi.org/10.1093/jat/bkv060.

43. Segawa H, Iwata YT, Yamamuro T, et al. Simultaneous chiral impurity analysis of methamphetamine and its precursors by supercritical fluid chromatography–tandem mass spectrometry. *Forensic Toxicol.* 2019;37(1):145-153, doi:https://doi.org/10.1007/s11419-018-0446-5.
44. Doi T, Asada A, Takeda A, et al. Enantioseparation of the carboxamide-type synthetic cannabinoids N-(1-amino-3-methyl-1-oxobutan-2-yl)-1-(5-fluoropentyl)-1H-indazole-3-carboxamide and methyl [1-(5-fluoropentyl)-1H-indazole-3-carbonyl]-valinate in illicit herbal products. *J Chromatogr A.* 2016;1473:83-89, doi:https://doi.org/10.1016/j.chroma.2016.10.049.
45. Andernach L, Pusch S, Weber C, et al. Absolute configuration of the synthetic cannabinoid MDMB-CHMICA with its chemical characteristics in illegal products. *Forensic Toxicol.* 2016;34(2):344-352, doi:https://doi.org/10.1007/s11419-016-0321-1.
46. Cannaert A, Franz F, Auwarter V, Stove CP. Activity-based detection of consumption of synthetic cannabinoids in authentic urine samples using a stable cannabinoid reporter system. *Anal Chem.* 2017;89(17):9527-9536, doi:https://doi.org/10.1021/acs.analchem.7b02552.
47. Cannaert A, Storme J, Franz F, Auwarter V, Stove CP. Detection and activity profiling of synthetic cannabinoids and their metabolites with a newly developed bioassay. *Anal Chem.* 2016;88(23):11476-11485, doi:https://doi.org/10.1021/acs.analchem.6b02600.
48. Noble C, Cannaert A, Linnet K, Stove CP. Application of an activity-based receptor bioassay to investigate the in vitro activity of selected indole- and indazole-3-carboxamide-based synthetic cannabinoids at CB1 and CB2 receptors. *Drug Test Anal.* 2019; 11: 501– 511, doi:https://doi.org/10.1002/dta.2517.
49. Wouters E, Walraed J, Robertson MJ, et al. Assessment of biased agonism among distinct synthetic cannabinoid receptor agonist scaffolds. *ACS Pharmacol Transl Sci.* 2019;3(2):285-295, doi:https://doi.org/10.1021/acsptsci.9b00069.
50. Banister SD, Longworth M, Kevin R, et al. Pharmacology of valinate and tert-leucinate synthetic cannabinoids 5F-AMBICA, 5F-AMB, 5F-ADB, AMB-FUBINACA, MDMB-FUBINACA, MDMB-CHMICA, and their analogues. *ACS Chem Neurosci.* 2016;7(9):1241-1254, doi:https://doi.org/10.1021/acschemneuro.6b00137.
51. Banister SD, Moir M, Stuart J, et al. Pharmacology of indole and indazole synthetic cannabinoid designer drugs AB-FUBINACA, ADB-FUBINACA, AB-PINACA, ADB-PINACA, 5F-AB-PINACA, 5F-ADB-PINACA, ADBICA, and 5F-ADBICA. *ACS Chem Neurosci.* 2015;6(9):1546-1559, doi:https://doi.org/10.1021/acschemneuro.5b00112.
52. Corbett WL, Inventor; Google Patents, assignee. Indole-3-carboxamides as glucokinase activators. 2005. Available at: https://patents.google.com/patent/US20040067939A1/en.
53. Pauli GF, Chen S-N, Simmler C, et al. Importance of purity evaluation and the potential of quantitative ^{1}H NMR as a purity assay: miniperspective. *J Med Chem.* 2014;57(22):9220-9231, doi:https://doi.org/10.1021/jm500734a.
54. Zhou Q, Yang D, Wu M, et al. Common activation mechanism of class A GPCRs. *Elife.* 2019;8:e50279, doi:https://doi.org/10.7554/eLife.50279.
55. Venkatakrishnan A, Ma AK, Fonseca R, et al. Diverse GPCRs exhibit conserved water networks for stabilization and activation. *Proc Natl Acad Sci.* 2019;116(8):3288-3293, doi:https://doi.org/10.1073/pnas.1809251116.

56. Wisler JW, Xiao K, Thomsen AR, Lefkowitz RJ. Recent developments in biased agonism. *Curr Opin Cell Biol.* 2014;27:18-24, doi:https://doi.org/10.1016/j.ceb.2013.10.008.
57. Hua T, Li X, Wu L, et al. Activation and signaling mechanism revealed by cannabinoid receptor-Gi complex structures. *Cell.* 2020;180(4):655-665. e618, doi:https://doi.org/10.1016/j.cell.2020.01.008.
58. Kumar KK, Shalev-Benami M, Robertson MJ, et al. Structure of a signaling cannabinoid receptor 1-G protein complex. *Cell.* 2019;176(3):448-458. e412, doi:https://doi.org/10.1016/j.cell.2018.11.040.
59. Hua T, Vemuri K, Nikas SP, et al. Crystal structures of agonist-bound human cannabinoid receptor CB 1. *Nature.* 2017;547(7664):468-471, doi:https://doi.org/10.1038/nature23272.
60. Schoeder CT, Hess C, Madea B, Meiler J, Müller CE. Pharmacological evaluation of new constituents of "Spice": synthetic cannabinoids based on indole, indazole, benzimidazole and carbazole scaffolds. *Forensic Toxicol.* 2018;36(2):385-403, doi:https://doi.org/10.1007/s11419-018-0415-z.
61. Krotulski AJ CA, Stove CP, Logan BK. The next generation of synthetic cannabinoids: Activity, toxicity, and proliferation of pent-4en and but-3en analogues including MDMB-4en-PINACA. *Drug Test Anal.* 2020, doi:https://doi.org/10.1002/dta.2935.
62. Janssens L, Cannaert A, Connolly MJ, Liu H, Stove CP. In vitro activity profiling of Cumyl-PEGACLONE variants at the CB1 receptor: Fluorination versus isomer exploration. *Drug Test Anal.* 2020, doi:https://doi.org/10.1002/dta.2870.
63. Banister SD, Adams A, Kevin RC, et al. Synthesis and pharmacology of new psychoactive substance 5F-CUMYL-P7AICA, a scaffold- hopping analog of synthetic cannabinoid receptor agonists 5F-CUMYL-PICA and 5F-CUMYL-PINACA. *Drug Test Anal.* 2019;11(2):279-291, doi:https://doi.org/10.1002/dta.2491.
64. Nickolls SA, Waterfield A, Williams RE, Kinloch RA. Understanding the effect of different assay formats on agonist parameters: a study using the μ-opioid receptor. *J Biomol Screen.* 2011;16(7):706-716, doi:https://doi.org/10.1177/1087057111406548.
65. Sachdev S, Vemuri K, Banister SD, et al. In vitro determination of the efficacy of illicit synthetic cannabinoids at CB_1 receptors. *Br J Pharmacol.* 2019;176(24):4653-4665, doi:https://doi.org/10.1111/bph.14829.
66. Weber C, Pusch S, Schollmeyer D, Münster-Müller S, Pütz M, Opatz T. Characterization of the synthetic cannabinoid MDMB-CHMCZCA. *Beilstein J Org Chem.* 2016;12:2808-2815, doi:https://doi.org/10.3762/bjoc.12.279.
67. Benredjem B, Gallion J, Pelletier D, et al. Exploring use of unsupervised clustering to associate signaling profiles of GPCR ligands to clinical response. *Nat Commun.* 2019;10(1):4075, doi:https://doi.org/10.1038/s41467-019-11875-6.
68. Gillis A, Gondin AB, Kliewer A, et al. Low intrinsic efficacy for G protein activation can explain the improved side effect profiles of new opioid agonists. *Sci Signal.* 2020;13(625):eaaz3140, doi:https://doi.org/10.1126/scisignal.aaz3140.
69. Wolff RF, Aune D, Truyers C, et al. Systematic review of efficacy and safety of buprenorphine versus fentanyl or morphine in patients with chronic moderate to severe pain. *Curr Med Res Opin.* 2012;28(5):833-845, doi:https://doi.org/10.1185/03007995.2012.678938.
70. Vandeputte MM, Cannaert A, Stove CP. In vitro functional characterization of a panel of non-fentanyl opioid new psychoactive substances. *Arch Toxicol.* 2020, doi:https://doi.org/10.1007/s00204-020-02855-7.

71. United Nations Office on Drugs and Crime. *Drug-related resolutions and decisions 2020 to 2029.* United Nations publications;2020 Available from: https://www.unodc.org/unodc/en/commissions/CND/Resolutions_Decisions/resolutions-and-decisions-2020-2029.html. Accessed: 06-06-2020
72. Centre for Forensic Science Research and Education. MMB-4en-PICA_101119_NMSLabs_Report. 2019; https://www.npsdiscovery.org/reports/monographs/.
73. Centre for Forensic Science Research and Education. 5F-EMB-PICA_061520_NMSLabs_Report. 2019; https://www.npsdiscovery.org/reports/monographs/.
74. Centre for Forensic Science Research and Education. 4F-MDMB-BICA_070120_NMSLabs_Report. 2019; https://www.npsdiscovery.org/reports/monographs/.
75. European Monitoring Centre for Drugs and Drug Addiction. *Formal notification of ethyl 2-[[1-(5-fluoropentyl)indole-3-carbonyl]amino]-3-methyl-butanoate (5F-EMB-PICA) as a new psychoactive substance under the terms of Regulation (EU) 2017/2101. EU-EWS-RCS-FN-2020-0020.* Luxembourg: Publications Office of the European Union;2020. Accessed: 03-06-2020
76. European Monitoring Centre for Drugs and Drug Addiction. *Formal notification of methyl 2-({[1-(4-fluorobutyl)-1H-indol-3-yl]carbonyl}amino)-3,3-dimethylbutanoate (4F-MDMB-BICA) as a new psychoactive substance under the terms of Regulation (EU) 2017/2101. EU-EWS-RCS-FN-2020-0019.* Luxembourg: Publications Office of the European Union;2020. Accessed: 03-06-2020
77. Norman C, McKirdy B, Walker G, Dugard P, Nic Daeid N, McKenzie C. Large-scale evaluation of ion mobility spectrometry for the rapid detection of synthetic cannabinoid receptor agonists in infused papers in prisons. *Drug Test Anal.* 2020;doi:https://doi.org/10.1002/dta.2945.

Table 1 Enantiospecific synthesis of 16 indazole- or indole-3-carboxamide synthetic cannabinoids. Compound numbering relates to that provided in Figure 1. The reagents are *N*-(3-dimethylaminopropyl)-*N′*-ethylcarbodiimide hydrochloride (EDC·HCl), 1-hydroxybenzotriazole hydrate (HOBt), diisopropyl amine (DIPEA) and the solvent is dimethyl sulfoxide (DMSO). The mixture was stirred at room temperature (r.t.) for 18 h.

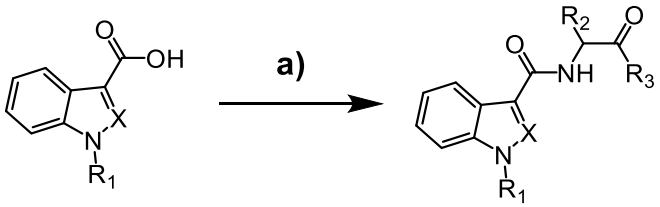

Reagents and conditions: a) appropriate amino acid, EDC·HCl, HOBt, DIPEA, DMSO, r.t., 18 h.

Compound	R_1	X	R_2	R_3	[amino acid]	Yield	Purity
(6) (*R&S*) 5F-MDMB-PICA	5-Fluoropentyl	CH	$CH(CH_3)_3$	OCH_3	[*tert*-Leucine methyl ester]	89.4 % & 87.9 %	>98.7 %
(7) (*R&S*) 4F-MDMB-BINACA	4-Fluorobutyl	N	$CH(CH_3)_3$	OCH_3	[*tert*-Leucine methyl ester]	94.2 % & 91 %	>99.7 %
(8) (*R&S*) MDMB-4en-PINACA	4-pentene	N	$CH(CH_3)_3$	OCH_3	[*tert*-Leucine methyl ester]	93.5 % & 88.0 %	>99.7 %
(11) (*R&S*) 5F-MMB-PINACA	5-Fluoropentyl	N	$CH(CH_3)_2$	OCH_3	[Valine methyl ester]	88.1 % & 84.4 %	>99.9 %
(14) (*R&S*) MMB-CHMICA	Cyclohexylmethyl	CH	$CH(CH_3)_2$	OCH_3	[Valine methyl ester]	81.1 % & 87.3 %	>99.6 %
(15) (*R&S*) MDMB-FUBINACA	4-Fluorobenzyl	N	$CH(CH_3)_3$	OCH_3	[*tert*-Leucine methyl ester]	84.7 % & 82.2 %	>99.9 %
(16) (*R&S*) MDMB-4en-PICA	4-pentene	CH	$CH(CH_3)_3$	OCH_3	[*tert*-Leucine methyl ester]	29.0 % &23.6 %	>99.7 %
(17) (*R&S*) MMB-4en-PICA	4-pentene	CH	$CH(CH_3)_2$	OCH_3	[*tert*-Leucine methyl ester]	38.3 % & 35.8 %	>99.7 %

Table 2 EC_{50} and E_{max} (relative to JWH-018, the reference) values at CB_1 as a measure of potency and efficacy, respectively, of valinate and *tert*-leucinate indole- and indazole-3-carboxamide enantiomer pairs in this and previous studies. Numbers in bold parenthesis refer to compound numbering provided in Figure 1.

	SCRA	CB_1 EC_{50} (nM) (± 95% CI)	(*R*)/(*S*) Potency Ratio	E_{max} (%) (± 95% CI)	Data Source	CB_1 EC_{50} (nM) (± 95% CI) [reference]	E_{max} (%) (± 95% CI) [reference]
	JWH-018	14.2 (7.61-27.9)	-	100 (90.1-112)	This Study	-	-
(6)	(*S*)-5F-MDMB-PICA	2.13 (0.685-5.61)	105	289 (259-325)		3.26 (2.07-5.15)[48]	331 (311-351)[48]
	(*R*)-5F-MDMB-PICA	224 (102-781)		121 (97.5-167)		-	-
(7)	(*S*)-4F-MDMB-BINACA	2.87 (1.10-7.71)	374	255 (222-289)		1.74 (1.22-2.49)[49]	253.6 (237-270)[49]*
	(*R*)-4F-MDMB-BINACA	1076 (497-2328)		128 (106-154)		-	-
(8)	(*S*)-MDMB-4en-PINACA	1.11 (0.54-2.26)	206	226 (203-253)		2.47 (1.19-5.27)[61]	239 (212-270)[61]
	(*R*)-MDMB-4en-PINACA	229 (141-397)		197 (176-220)		-	-
(11)	(*S*)-5F-MMB-PINACA	7.99 (4.22-13.0)	11.6	202 (185-221)		15.1 (10.2-23.9)[23]	259 (238-287)[23]
	(*R*)-5F-MMB-PINACA	93.0 (63.1-126)		193 (178-210)		-	-
(14)	(*S*)-MDMB-FUBINACA	0.245 (0.0786-0.667)	364	248 (218-282)		0.36 (0.17-0.69)[23]	241 (221-263)[23]
	(*R*)-MDMB-FUBINACA	89.2 (40.5-178)		127 (106-151)		-	-
(15)	(*S*)-MMB-CHMICA	9.51 (5.11-19.5)	8.03	254 (225-299)		-	-
	(*R*)-MMB-CHMICA	76.4 (39.8-140)		253 (225-281)		-	-
(16)	(*S*)-MDMB-4en-PICA	3.70 (2.21-6.13)	74.8	289 (259-325)		11.5 (5.12-33.2)[61]	302 (256-391)[61]
	(*R*)-MDMB-4en-PICA	277 (154-494)		49.8 (44.0-55.9)		-	-
(17)	(*S*)-MMB-4en-PICA	149 (80.9-290)	3.23	172 (154-191)		125 (64.6-332)[61]	191 (163-237)[61]
	(*R*)-MMB-4en-PICA	481 (183-1161)		76.4 (39.8-140)		-	-
	JWH-018	45.1 (32.4-62.9)	-	103 (97.1-109)	[24]	-	-
(1)	(*S*)-AB-FUBINACA	12.9 (10.1-18.1)	115	283 (265-302)		15.6 (10.4-23.2)[48]	324 (302-346)[48]
	(*R*)-AB-FUBINACA	1480 (977-4770)		90.2 (78.6-127)		-	-
(4)	(*S*)-MMB-FUBINACA	9.11 (6.07-14.1)	6.12	267 (247-293)		-	-
	(*R*)-MMB-FUBINACA	55.8 (39.3-78.1)		154 (144-164)		-	-
(5)	(*S*)-5F-MDMB-PINACA	1.78 (0.72-4.11)	73.1	331 (293-406)		0.84 (0.52-1.24)[23] 0.18 (0.13-0.27)[49]	319 (291-354)[23] 250 (236-264)[49]*
	(*R*)-5F-MDMB-PINACA	131 (98.6-174)		180 (170-190)		-	-
(13)	(*S*)-AB-CHMINACA	6.16 (4.49-8.55)	51.8	324 (307-344)		3.45 (1.96-6.14)[23]	391 (358-435)[23]
	(*R*)-AB-CHMINACA	319 (242-420)		113 (107-119)		-	-

*: E_{max} in the referenced paper was calculated in reference to CP55940. For comparability, these numbers were recalculated in reference to JWH-018.

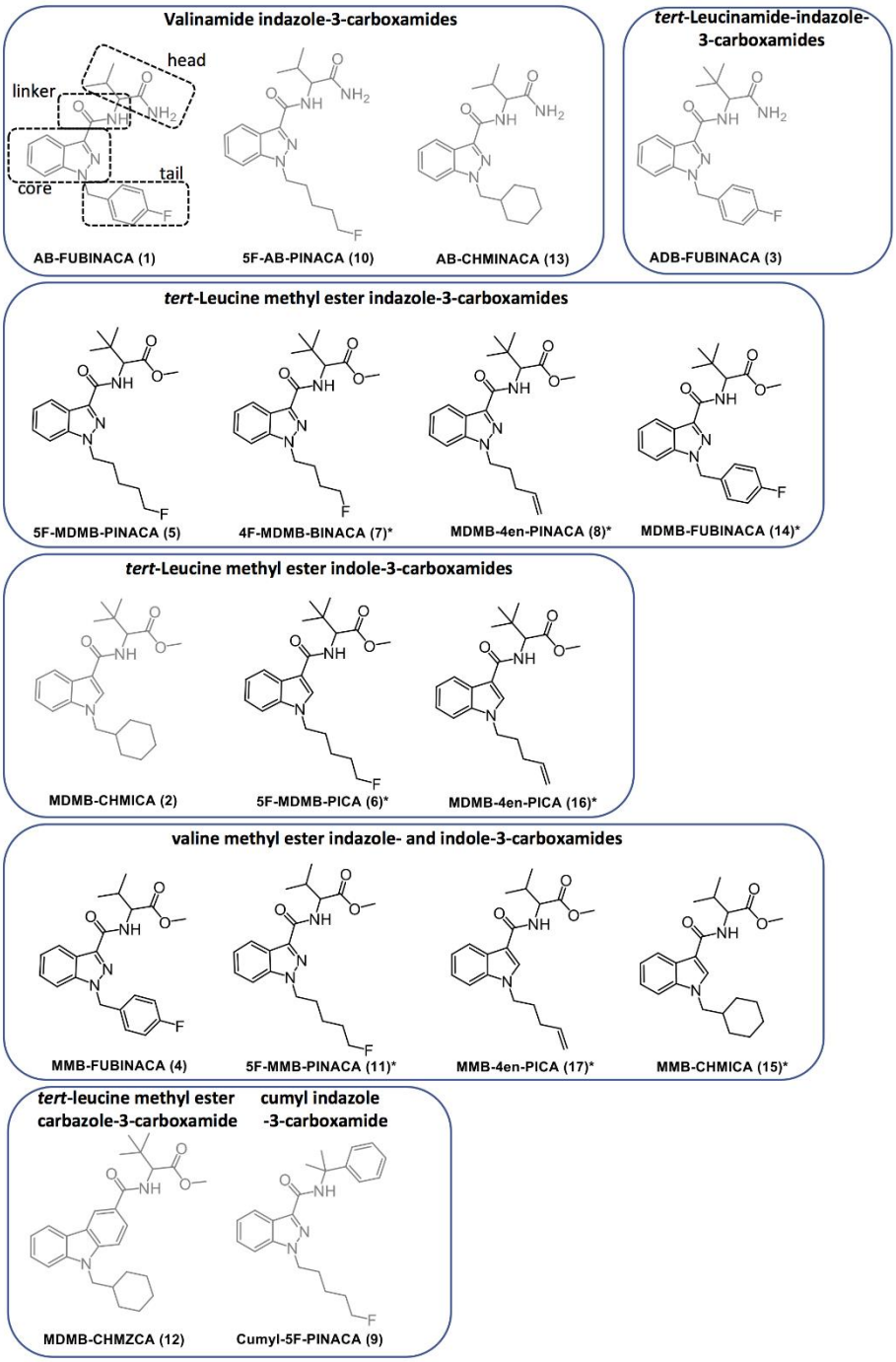

Figure 1: Structures of AB-FUBINACA **(1)**, MDMB-CHMICA **(2)**, ADB-FUBINACA **(3)**, MMB-FUBINACA **(4)**, 5F-MDMB-PINACA **(5)**, 5F-MDMB-PICA **(6)**, 4F-MDMB-BINACA **(7)**, MDMB-4en-PINACA **(8)**, Cumyl-5F-PINACA **(9)**, 5F-AB-PINACA **(10)**, 5F-MMB-PINACA **(11)**, MDMB-CHMZCA **(12)**, AB-CHMINACA **(13)**, MDMB-FUBINACA **(14)**, MMB-CHMICA **(15)**, MDMB-4en-PICA **(16)** and MMB-4en-PICA **(17)**. Chiral centers are identified with an asterisk on the structure and compounds with stars after the name were synthesized during this study. The compounds are grouped together based on their structural class, as is indicated by the boxes. Compounds that were synthesized as part of this study and our previous study[24] are colored black whereas compounds that are mentioned in the text, but were not synthesized are colored grey.

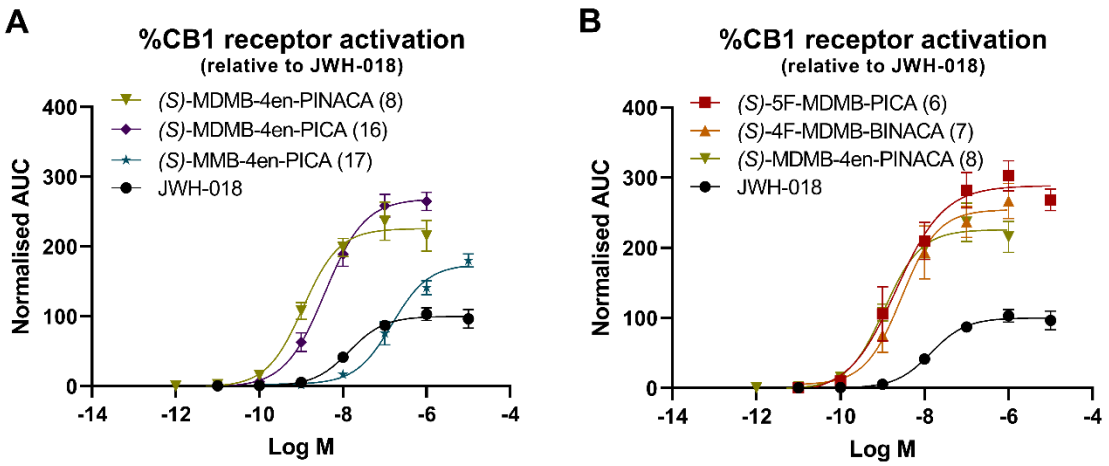

Figure 2: Concentration-dependent interaction of CB_1 with βarr2 upon stimulation with (a) (*S*)-enantiomers of SCRAs with alkene-type tails and the (b) most prevalent SCRAs currently detected in Scottish prisons. AUC, area under the curve (luminescence over time). Data are given as mean receptor activation ± SEM (n = 3), normalized to the E_{max} of JWH-018 (= 100 %). Numbers in parenthesis refer to compound numbering provided in Figure 1.

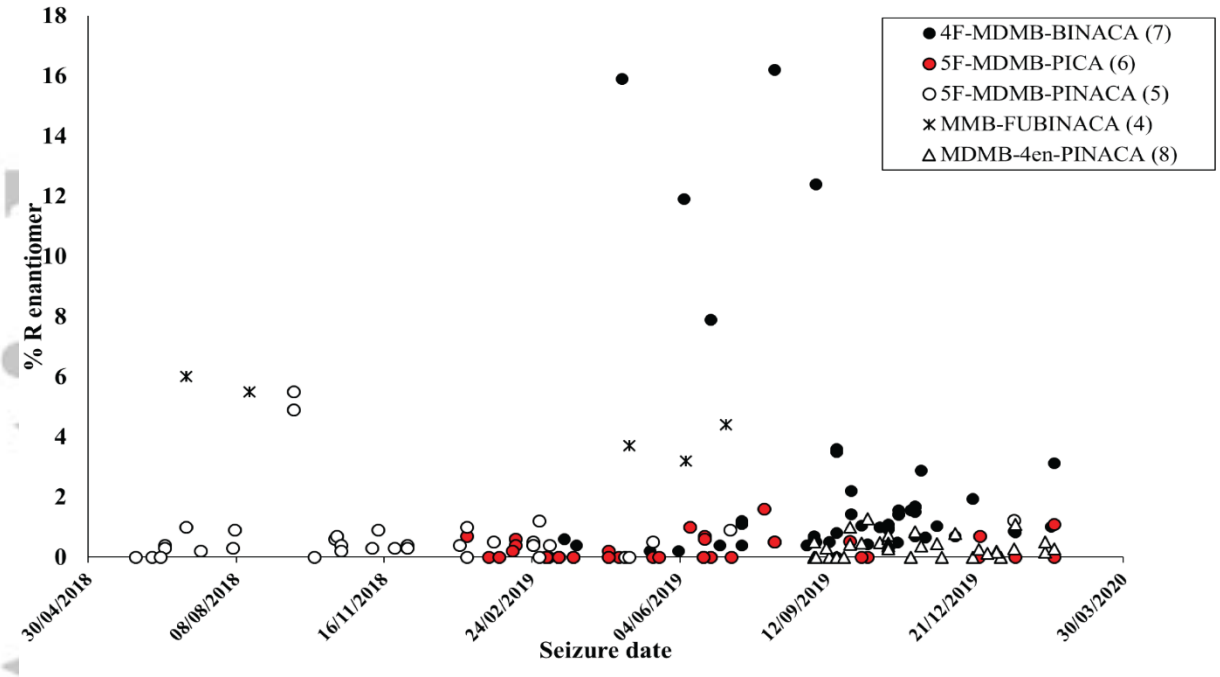

Figure 3: Chiral profiling data (% (*R*)-enantiomer detected) for SCRAs in infused paper samples seized in Scottish prisons between June 2018 and February 2020. Number of detections: MMB-FUBINACA **(4)**, n = 5; 5F-MDMB-PINACA **(5)**, n= 36 (4 detections not included due to missing seizure dates); 5F-MDMB-PICA **(6)**, n = 42 (13 detections not included due to missing seizure dates); 4F-MDMB-BINACA **(7)**, n = 57 (4 detections not included due to missing seizure dates); MDMB-4en-PINACA, n = 45 (4 detections not included due to missing seizure dates). Numbers in parenthesis refer to compound numbering provided in Figure 1.

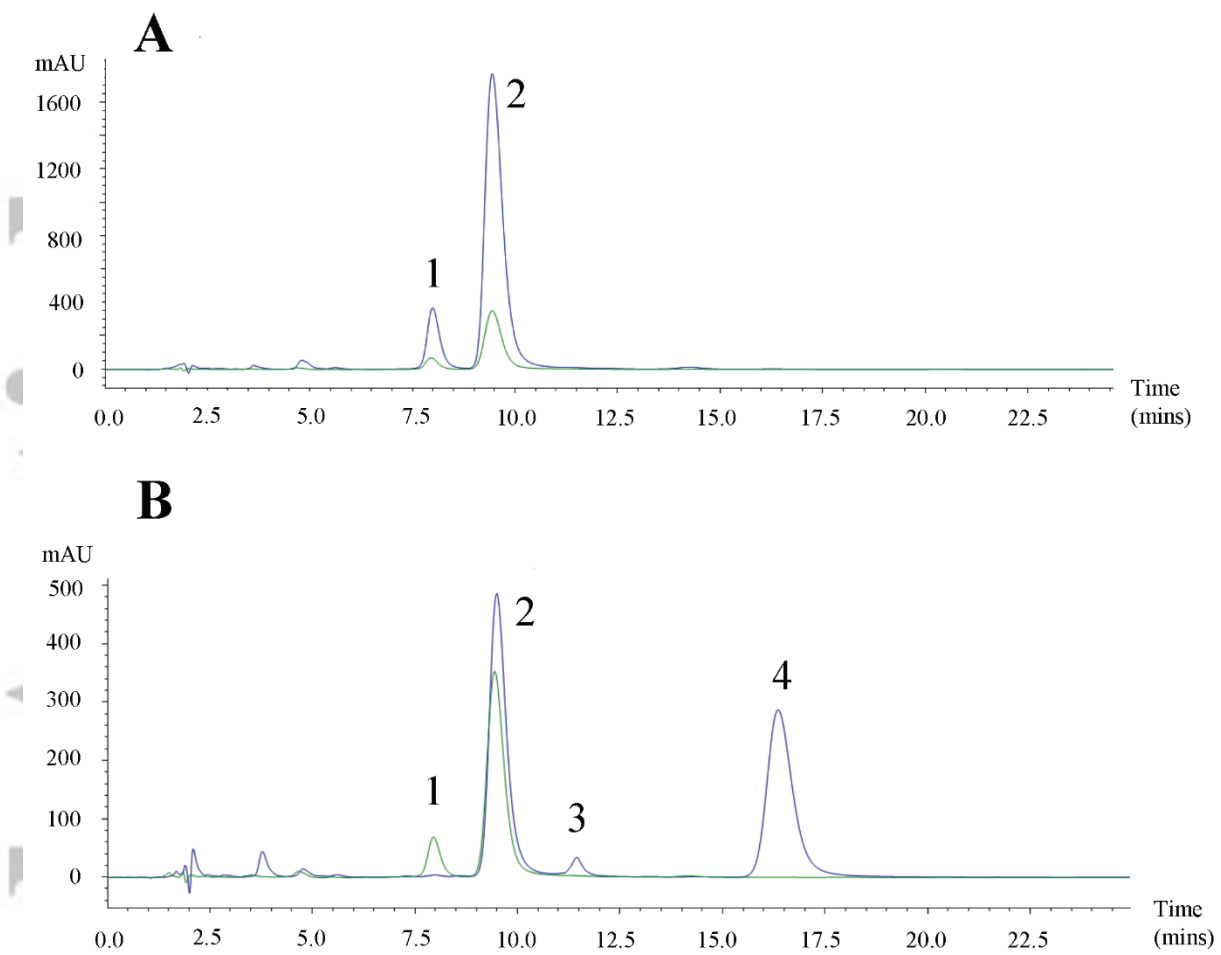

Figure 4: (a) Overlaid HPLC-PDA chromatogram for sample FL19/0224-2 (1 µL (green) and 5 µL (blue) injections; (b) Overlaid HPLC-PDA chromatograms for 1µL injections of samples FL19/0224-2 (green) and FL19/0215-G (blue). Peak Identification – 1: (*R*)-4F-MDMB-BINACA **(7)**, 2: (*S*)-4F-MDMB-BINACA **(7)**, 3: (*S*)-5F-MDMB-PICA **(6)**, 4: (*S*)-MDMB-4en-PINACA **(8)**. Numbers in parenthesis refer to compound numbering provided in Figure 1.

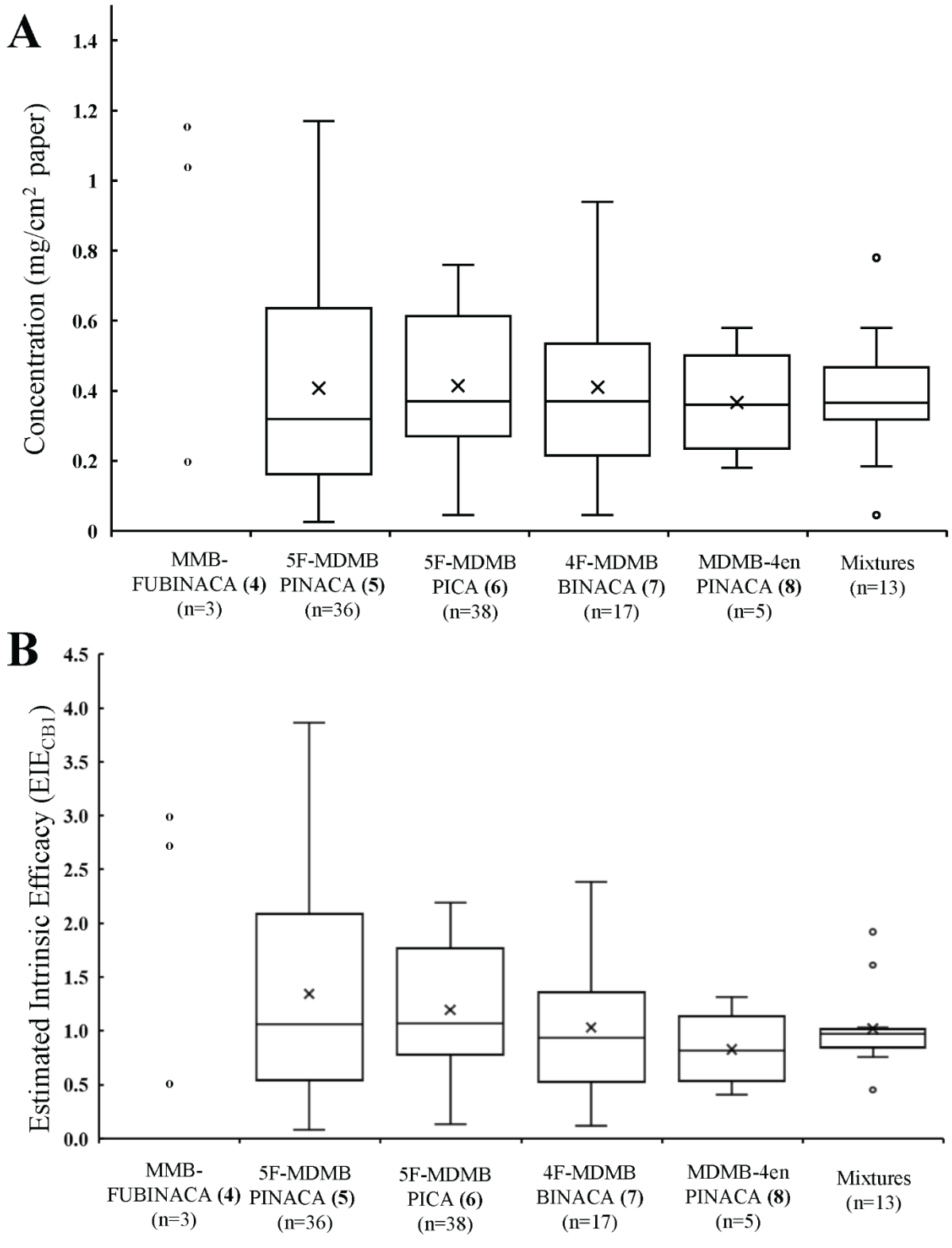

Figure 5: (a) Summary of SCRA concentrations detected in infused papers seized in Scottish prisons June 2018-September 2019 for samples where chiral profiling data is also available; (b) Summary of estimated intrinsic CB_1-mediated potency (EIE_{CB1}) data for infused papers seized in Scottish prisons June 2018-September 2019. Numbers in parenthesis refer to compound numbering provided in Figure 1.

The pharmacology of a group of 16 enantiopure carboxamide-type SCRAs is examined and a chiral chromatography method to analyse a large group of seized prison samples is applied. The potency, efficacy, concentration and enantiopurity of the individual SCRAs all contribute to the overall potency and efficacy of seized samples.

Example from DTA on next page

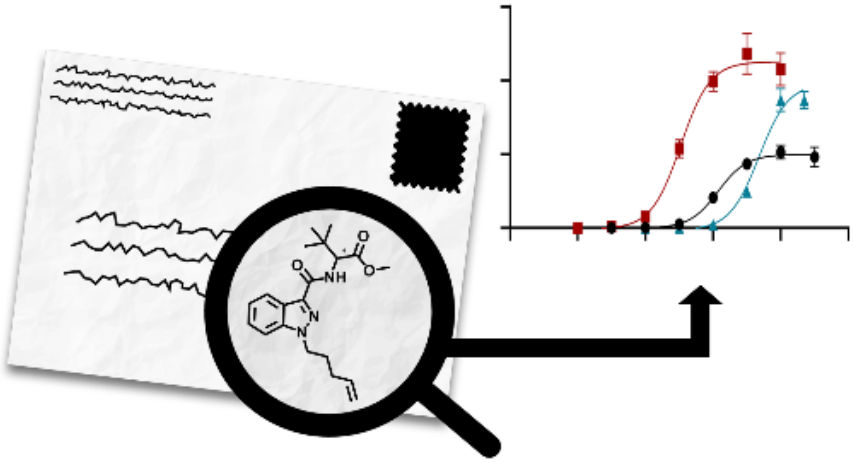

Shape Matters: The Application of Activity-Based In Vitro Bioassays and Chiral Profiling to the Pharmacological Evaluation of Synthetic Cannabinoid Receptor Agonists in Drug-Infused Papers Seized in Prisons

Lysbeth H. Antonides[1], Annelies Cannaert[2], Caitlyn Norman[1], Niamh Nic Daeid[1], Oliver B. Sutcliffe[3], Christophe P. Stove[2*], Craig McKenzie[1*]

Graphical Table of Contents

DTA's table of contents will be presented in graphical form with a brief abstract.

The table of contents entry must include the article title, the authors' names (with the corresponding author indicated by an asterisk), no more than 80 words or 3 sentences of text summarising the key findings presented in the paper and a figure that best represents the scope of the paper. (see the section on abstract writing for more guidance).

Table of contents entries should be submitted to Manuscript Central in one of the generic file formats and uploaded as 'Supplementary material for review' during the initial manuscript submission process.

The image supplied should fit within the dimensions of 50mm x 60mm, and be fully legible at this size.

Examples for arranging the text and figures as well as paper title and authors' names are shown below.

Detection assays for drugs and methods of sports doping published between 2007 and 2008 are critically reviewed and evaluated in context with the Prohibited List 2008 as established by the World Anti-Doping Agency.

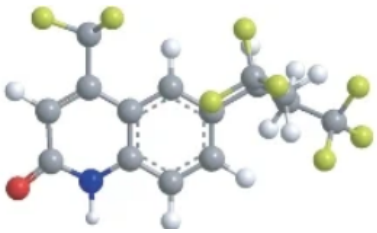

Annual banned-substance review: the Prohibited List 2008 analytical approaches in human sports drug testing

Mario Thevis, Tiia Kuuranne, Hans Geyer and Wilhelm Schänzer